1968

Estimation of bending moments in box-beam bridges using cross-sectional deflections, June 1968,

S. J. Fang

M. A. Macias-Rendon

D. A. VanHorn

LEHIGH UNIVERSITY INSTITUTE OF RESEARCH

ESTIMATION OF BENDING MOMENTS IN BOX-BEAM BRIDGES USING CROSS-SECTIONAL DEFLECTIONS

by

Shu-jin Fang

Miguel A. Macías Rendón

David A. VanHorn

Fritz Engineering Laboratory Report No. 322.2

Project 322

A STRUCTURAL MODEL STUDY
OF LOAD DISTRIBUTION IN HIGHWAY BRIDGES

Progress Reports Completed to Date

Progress Report No.	
1	A STRUCTURAL MODEL STUDY OF LOAD DISTRIBUTION IN BOX-BEAM BRIDGES. Macías Rendón, M. A. and VanHorn, D. A., F. L. Report 322.1, May 1968
2	ESTIMATION OF BENDING MOMENTS IN BOX-BEAM BRIDGES USING CROSS-SECTIONAL DEFLECTIONS. Fang, S. J., Macías Rendón, M. A. and VanHorn, D. A., F. L. Report 322.2, June 1968

ESTIMATION OF BENDING MOMENTS IN BOX-BEAM BRIDGES USING CROSS-SECTIONAL DEFLECTIONS

by

Shu-jin Fang

Miguel A. Macías Rendón

David A. VanHorn

This work was conducted as part of the project "A Structural Model Study of Load Distribution in Highway Bridges", sponsored by the National Science Foundation. The opinions, findings, and conclusions expressed in this report are those of the writers and not necessarily those of the sponsors.

Department of Civil Engineering

Fritz Engineering Laboratory

Lehigh University

Bethlehem, Pennsylvania

June 1968

Fritz Engineering Laboratory Report No. 322.2

TABLE OF CONTENTS

ABSTRACT

This report describes part of the research work conducted under the Fritz Laboratory Project 322, entitled "A Structural Model Study of Load Distribution in Highway Bridges".

The purposes of this work were to:

1. Find an analytical correlation between the transverse distributions of longitudinal bending moments and the cross-sectional deflections in box-beam bridges.
2. Develop a practical method for the estimation of bending moments in box-beam bridges by the use of cross-sectional deflections.

To experimentally verify the proposed method, test results from seventeen small scale (1/16) Plexiglas box-beam bridge models are reported. Details of the fabrication, instrumentation and testing of the models can be found in Ref. 9. In particular, it should be noted that these seventeen Plexiglas models were tested under static vehicular loads, using the creep compensating technique.

An analysis of the experimental results and a proposed method for estimating bending moments are presented. The estimated

values exhibit good agreement with the model test results. The contribution of curbs and parapets to the flexural stiffness of the bridge was taken into account in the analysis. The influences on the correlation between bending moments and cross-sectional deflections due to curbs, parapets, diaphragms, size and spacing of beams, and thickness of slab are discussed.

The proposed method was used to estimate bending moments in one existing bridge. The estimated values were found to be close to those obtained in the field test. As a result of this investigation, it is believed that the use of measured deflections, along with the geometric properties of the cross-section, may enable an economical and accurate estimation of the lateral load distribution in prestressed concrete box-beam bridges.

1. INTRODUCTION

1.1 Background

Bridge structures form one of the most important components of modern highway systems. Over the past fifteen years, many new concepts have been introduced in the area of bridge design. One of the more recent concepts was the design of beam-slab bridges utilizing precast, prestressed concrete box beams, spread apart and equally spaced, along with a cast-in-place concrete slab. The curbs and parapets are also cast in place, using reinforcing bars in the connection with the slab. In bridges of this type constructed in Pennsylvania, the beams are designed according to the provisions set forth in the Pennsylvania Department of Highways Bridge Division Standards ST-200 through ST-208.[13] These provisions closely parallel those covering the design of longitudinal beams as set forth in the A.A.S.H.O. Standard Specifications for Highway Bridges.[1]

1.2 Object and Scope

Recently, the field tests of several in-service highway bridges have established the fact that the actual distribution of maximum vehicular loads to the beams is not in line with the distribution assumed in the design.[5] In these tests, strain gages attached to the superstructure at selected locations were used to evaluate the load distribution.

To approach the evaluation in a different way, this investigation is directed toward the possible correlation of the transverse distribution of bending moment in the longitudinal beams with the cross-sectional deflections. The principal advantage of using cross-sectional deflections to evaluate the bending moments is that there are considerably fewer problems associated with the installation and operation of deflection equipment than with strain gage recording equipment. Equally important is the fact that the deflections are a form of an integrated response of the entire structure; while the fiber strains are of a more local nature, and greatly affected by singularities in the immediate vicinity of the strain measurement. If a fine correlation between the bending moments and deflections can be found, the primary use of deflections in field studies and laboratory work could result in more economical and efficient testing methods.

The principal objectives of the study presented in this report are:

1. To find a theoretical correlation between the transverse distribution of

bending moment in the longitudinal beams and the cross-sectional deflections, in prestressed concrete spread box-beam bridges, with or without curbs, parapets, and diaphragms.

2. To develop a practical method of estimating the individual bending moments by using the cross-sectional deflections. The deflection of each box beam can be either directly measured by dial gages or by deflectometers, or even calculated by one of the existing theories of analysis.[10]

The study presented in this report is a part of the research work conducted under the Fritz Laboratory Project 322, entitled "A Structural Model Study of Load Distribution in Highway Bridges". The primary objective of the overall project is the investigation of static live load distribution in prestressed concrete spread box-beam bridges.

In order to experimentally verify the analytical correlation and the proposed method, presented in Chapters 2 and 5, respectively, a systematic series of seventeen small scale (1/16) Plexiglas box-beam bridge models was designed and fabricated, assembled and tested. Comparisons of the distributions of experimental bending moments with experimental cross-sectional deflections and with estimated distributions of bending moments are given in this report. In addition, the influence of curbs, parapets, size and spacing of beams, and thickness of slab, on the correlation between bending moments and cross-sectional deflections, is discussed in detail.

1.3 Previous Research

A number of field investigations have been conducted on highway bridges of the beam-slab type. Most of the bridges tested were I-beam bridges with either steel or prestressed concrete beams. Only a limited number of studies have dealt with prestressed concrete box-beam bridges. In particular, relatively little experimental and theoretical work has been carried out in the study of simply-supported, spread box-beam bridges.

An extensive annotated bibliography on lateral distribution of loads in bridges, including slab bridges and beam-slab bridges, is given in Ref. 14. Since the information presented herein is evaluated by model tests, some of the previous model studies on load distribution are included as Refs. 2, 3, 4, 6, 7, 8, 11, 15, 16, 18, and 19.

2. THEORETICAL ANALYSIS

2.1 Statement of Problem

In the theoretical work presented in Ref. 17, a single distribution coefficient was established for the determination of both deflections and longitudinal bending moments in a beam-slab bridge. This single distribution coefficient was applied only to bridge cross-sections with equal stiffness in all of the beams, and curb and parapet were not considered.

Satisfactory agreement with the theory was found in tests reported in Refs. 7 and 8 where, after a careful comparison of the theoretical distribution coefficients for longitudinal bending moments with the experimental distribution coefficients, it was concluded that the agreement was acceptable. Furthermore, an excellent agreement was found in the comparisons between the theoretical and experimental distribution coefficients for deflections.

On the other hand, the previous conclusions were not agreed upon by other investigators. Comparison of the strains in the bottom flanges of I beams with the deflections in a beam-slab bridge showed no consistent correlation.[6] The same problem was observed in Ref. 12, where it was concluded that the bending moments and the deflections in the beams are not proportional as determined from field test results. It was also pointed out in Ref. 11 that there is a considerable discrepancy between the experimental distribution of bending moments and the calculated distribution coefficients, based on a sinusoidal longitudinal distribution of a concentrated load. Thus, an approximate adjustment to the Guyon-Massonnet theory was proposed,[11] in order to take into account the effect of a concentrated load.

Confusion may arise from the fact that different conclusions were reached by several investigators. Therefore, some of the assumptions in the theory will be examined.

The Guyon-Massonnet method[5] is based on the following two main assumptions:

1. That a constant stiffness exists in both the longitudinal and transverse directions. In other words, the effects of a stiffening edge member and beams of different size cannot be considered.
2. That the transverse distribution of actual concentrated loads is the same as the transverse distribution of loads which are distributed sinusoidally along the length of the bridge.

It is a fact that most of the existing prestressed concrete bridges have curbs and parapets. Test results have shown that some composite action exists between curbs and beams, and between curbs and parapets.[5] Thus, the first assumption cannot be satisfied when the curbs and parapets are present. If the effects due to curbs and parapets are not accounted for, errors will be introduced.

In addition, there is a substantial difference between the actual single concentrated load and the assumed sinusoidal load varying along the bridge. This difference is one of the reasons for the disagreement between the theoretical distribution coefficients for bending moments and experimentally determined values. Finally, the assumption of Poisson's ratio equal to zero is another source of error in the method under discussion.

Furthermore, it is believed that it is not adequate to use the strains at the bottom face of beams as a direct indication of bending moments in beams.[4,7] The evaluation of the true bending moment in the beams should take into account the contribution of the individual slabs, since equilibrium should exist in each beam-slab unit. To more accurately determine the bending moments in beam-slab units, the strains along the side faces of beams, top of slab, curbs, and parapets should be measured carefully, as well as the strains on the bottom faces of beams.

In order to better understand the correlation between the transverse distributions of longitudinal bending moments and the cross-sectional deflections in a single span, simply-supported box-beam bridge in which curbs and parapets may or may not be present, a theoretical analysis is given in this chapter. Finally, a simplified method of estimating bending moments in the beams by using the cross-sectional deflections and geometrical configuration of the cross-section of the bridge is proposed in Chapter 5.

2.2 Assumptions

Before the analysis can be developed, the following assumptions are made.

1. The structure is homogeneous and isotropic before the occurrence of any cracking (both in longitudinal and transverse directions) or excessive deformation.
2. The thickness of each plate component is assumed to be constant and uniform.
3. A linear relationship exists between forces and deflections. Only elastic

behavior of the bridge is considered in the analysis.

4. A full composite action exists between beams, slab, curbs, and parapets. All connections insure that no relative displacements between components can occur.

5. The end supports provide no longitudinal restraint for each beam-slab unit.

6. The bending moment diagrams of all beam-slab units are assumed similar in geometry.

7. The secondary effects on the deflection of the beams due to twisting are negligible.

8. The transverse bending moments (with respect to a vertical axis) in beam-slab units are assumed to be small compared with the longitudinal bending moments (with respect to horizontal axis) and can be neglected.

9. The presence of diaphragms does not affect the analysis.

2.3 Development

A simply-supported, box-beam bridge can be regarded as an assemblage of a set of beam-slab units. Each beam-slab unit is composed of a box beam and an individual width of slab. Curbs and parapets act in combination with the exterior beam-slab units. By Assumption 9, midspan and end diaphragms, which are originally designed in order to improve the load distribution of the bridge, are not considered in this analysis. It is believed that the diaphragms will not substantially affect the correlation between the transverse distributions of longitudinal bending moments and distributions of cross-sectional deflections. This concept will be discussed in Chapter 5.

A typical cross-section of a box-beam bridge is given in Fig. 1a. When the deck of the bridge is subjected to a vehicular load, five internal forces and moments are produced in any cross-section of each beam-slab unit. These forces and moments are longitudinal bending moment M_x, transverse bending moment M_y, total vertical shear force S_y, total horizontal shear force S_x, and twisting moment M_{xy}, which is shown in Fig. 1b.

The vertical deflection at the centroid, δ_y, of given beam-slab unit can be written as

$$\delta_y = (\delta_y)_{bending} + (\delta_y)_{shear} + (\delta_y)_{torsion} \qquad (1)$$

As a beam-slab unit has a box beam of rigid closed cross-section, it is reasonable to consider the unit as a solid beam insofar as its behavior under the combined flexure and torsion is concerned.

Consequently, the cross-section of each beam-slab unit which is initially plane remains plane after deformation, and there is no extension or shearing strain in the plane of the cross-section. Saint Venant's principle is valid in this case. According to this principle and the adopted hypothesis, the internal forces acting on the cross-section lead to one resultant, which may be replaced by an equivalent system of forces without changing the state of strain of the mathematical model adopted for the solid beam. The beam-slab unit would undergo torsion according to the law of pure torsion. Since the effect of the vertical deflection due to pure torsion is neglected according to Assumption 7, and since the effect of shear force is very small, Eq. 1 can be simplified as

$$\delta_y \cong (\delta_y)_{bending}$$

considering a beam-slab unit as simply supported at both ends, (Assumption 5), the vertical deflection at the centroid of a given section due to bending can be found from Fig. 1b as follows:

The deflection in the VV direction is

$$\delta_{vv} = F\left(\frac{M_{uu}}{E\,I_{uu}}\right)$$

and the deflection in the UU direction is

$$\delta_{uu} = F\left(\frac{M_{vv}}{E\,I_{vv}}\right)$$

where M_{uu} and M_{vv} are the bending moments with respect to Axes UU and VV, respectively,

I_{uu} and I_{vv} are the moments of inertia with respect to Axes UU and VV, respectively,

and F is a certain function depending on the bending moment diagram and on the position of the section.

Superimposing the vertical components of δ_{vv} and δ_{uu}, the total vertical deflection is

$$\delta_y = \delta_{uu} \operatorname{Sin} \theta + \delta_{vv} \operatorname{Cos} \theta$$

$$= F\left(\frac{M_{vv}}{E\,I_{vv}}\right) \operatorname{Sin} \theta + F\left(\frac{M_{uu}}{E\,I_{uu}}\right) \operatorname{Cos} \theta \qquad (2)$$

By the law of transformation of coordinate axes, the moments of inertia I_{uu}, I_{vv}, and I_{uv} are expressed in terms of I_{xx}, I_{yy}, and I_{xy}.

$$\begin{bmatrix} I_{uu} & -I_{uv} \\ -I_{uv} & I_{vv} \end{bmatrix} = R \begin{bmatrix} I_{xx} & -I_{xy} \\ -I_{xy} & I_{yy} \end{bmatrix} R^T \tag{3}$$

wherein R is the rotation matrix

and

$$R = \begin{bmatrix} \text{Cos}\ \theta & -\text{Sin}\ \theta \\ -\text{Sin}\ \theta & \text{Cos}\ \theta \end{bmatrix}$$

Substituting R into Eq. 3, we obtain

$$\begin{aligned} I_{uu} &= I_{xx}\ \text{Cos}^2\ \theta + I_{yy}\ \text{Sin}^2\ \theta - 2\, I_{xy}\ \text{Sin}\ \theta \cdot \text{Cos}\ \theta \\ I_{yy} &= I_{xx}\ \text{Sin}^2\ \theta + I_{yy}\ \text{Cos}^2\ \theta + 2\, I_{xy}\ \text{Sin}\ \theta \cdot \text{Cos}\ \theta \\ I_{uv} &= (I_{yy} - I_{xx})\ \text{Sin}\ \theta\ \text{Cos}\ \theta - I_{xy}\ \text{Cos}\ (2\theta) \end{aligned} \tag{4}$$

M_{uu} and M_{vv} can be expressed as

$$\begin{aligned} M_{uu} &= M_x\ \text{Cos}\ \theta + M_y\ \text{Sin}\ \theta \\ M_{vv} &= -M_x\ \text{Sin}\ \theta + M_y\ \text{Cos}\ \theta \end{aligned} \tag{5}$$

Substituting Eqs. 4 and 5 into Eq. 2

$$\delta_y = \frac{F}{E}\left(\frac{M_x \cos\theta + M_y \sin\theta}{I_{xx}\cos^2\theta + I_{yy}\sin^2\theta - 2 I_{xy}\sin\theta\cos\theta}\right)\cos\theta$$

$$+ \frac{F}{E}\left(\frac{-M_x \sin\theta + M_y \cos\theta}{I_{xx}\sin^2\theta + I_{yy}\cos^2\theta + 2 I_{xy}\sin\theta\cos\theta}\right)\sin\theta \qquad (6)$$

According to Assumption 8, Eq. 6 can be simplified as

$$\delta_y = F\frac{M_x}{E}\left(\frac{\cos^2\theta}{I_{xx}\cos^2\theta + I_{yy}\sin^2\theta - 2 I_{xy}\sin\theta\cos\theta}\right.$$

$$\left. - \frac{\sin^2\theta}{I_{xx}\sin^2\theta + I_{yy}\cos^2\theta + 2 I_{xy}\sin\theta\cos\theta}\right) \qquad (7)$$

Setting

$$I_{eq} = \frac{1}{\dfrac{\cos^2\theta}{I_{xx}\cos^2\theta + I_{yy}\sin^2\theta - I_{xy}\sin(2\theta)} - \dfrac{\sin^2\theta}{I_{xx}\sin^2\theta + I_{yy}\cos^2\theta + I_{xy}\sin(2\theta)}} \qquad (8)$$

wherein, I_{eq} is defined as "Equivalent Moment of Inertia" for each beam-slab unit. If $\theta = 0$, $I_{eq} = I_{xx}$.

Substituting Eq. 8 into Eq. 7 and rearranging, we obtain

$$M_x = \frac{(E\, I_{eq})\ \delta_y}{F} \qquad (9)$$

This is the expression for the longitudinal bending moment at a cross-section of a beam-slab unit.

Considering the equilibrium condition of longitudinal bending moments at any chosen cross-section of the bridge

$$(M_x)_{EXT.} = (M_x)_{INT.} = \sum_{i=1}^{i=m} (M_x)_i = \sum_{i=1}^{i=m} \frac{E_i \ (I_{eq})_i}{F_i} (\delta_y)_i \tag{10}$$

where $(M_x)_{EXT.}$ = total external bending moment

$(M_x)_{INT.}$ = total internal resisting bending moment

m = number of beams

i = subscript used to identify beam-slab units

By definition, the moment percentage (M.P.) is

$$(M.P.)_i = \frac{(M_x)_i}{\sum_{i=1}^{i=m} (M_x)_i} \times 100$$

Using Eq. 10

$$(M.P.)_i = \frac{\frac{E_i\ (I_{eq})_i}{F_i}\ (\delta_y)_i}{\sum_{i=1}^{i=m} \frac{E_i\ (I_{eq})_i}{F_i}\ (\delta_y)_i} \times 100$$

According to Assumptions 1 and 6, E_i and F_i are the same for all beam-slab units; therefore, a correlation between the transverse distribution of longitudinal bending moments in beam-slab units and the cross-sectional deflections is found as follows:

$$(M.P.)_i = \frac{(I_{eq})_i\ (\delta_y)_i}{\sum_{i=1}^{i=m} (I_{eq})_i\ (\delta_y)_i} \tag{11}$$

For the special case when $(I_{eq})_i$ is the same for all beam-slab units, Eq. 11 becomes

$$(M.P.)_i = \frac{(\delta_y)_i}{\sum_{i=1}^{i=m} (\delta_y)_i} = (D.P.)_i \tag{12}$$

In other words, the moment percentages (M.P.) will be equal to the deflection percentages (D.P.), if the bridge has identical equivalent moments of inertia for all beam-slab units.

3. EXPERIMENTAL STUDY

3.1 General Consideration

In this chapter, brief descriptions of the test program and tested models used in this study are presented. Details concerning the construction, instrumentation, fabrication, and modeling techniques of the models, as well as the similitude requirements considered, can be found in Ref. 9.

3.2 Test Program

The test program for the models was designed with the objectives mentioned in Section 1.2.

In the experimental model investigation, a series of seventeen 1/16-scale Plexiglas models was fabricated and tested. All of the bridges were simply supported over a span of 48.94 inches.

According to the method of fabrication, the models can be classified into two categories: (1) Glued model, in which all of the components were cemented together using Ethylene Dichloride, and (2) Bolted model, in which pre-fabricated beams, slab, curbs, parapets, and diaphragms were connected together by screws or tie-rods. A brief description of all models is shown in Table 1.

According to the geometry of the cross-section, the models can be separated into two groups: one group of models without curbs and parapets, and the other with curbs and parapets. Within each group, bridges can again be divided into two sub-groups: (1) bridges with diaphragms, and (2) bridges without diaphragms. For the convenience of simple use in later chapters, it might be helpful to classify the bridges as follows:

1. Case (0,0,0) represents bridges without curbs, parapets, and diaphragms, such as models B1, B5, B9, B15, and B16.
2. Case (0,0,1) represents bridges without curbs and parapets, but with diaphragms, such as models B2, B6, and B10.
3. Case (1,1,0) represents bridges without diaphragms, but with curbs and parapets, such as models B3, B7, and B11.
4. Case (1,1,1) represents bridges with all elements. Most real bridges belong to this category. Models A1, B4, B8, B12, B13, and B14 are in this case.

Bridge model B4 was chosen as the typical bridge in this study. The cross-sectional dimensions are shown in Fig. 1a. The five loading lanes covering the entire clear width of 20.88 inches of the roadway, are numbered 1 through 5 from the east edge, westward. Four identical box beams, representing prototype beams 4 feet wide and 39 inches deep. A longitudinal view of a bolted model is given in Fig. 2, and the arrangement of all basic cross-sections of models is shown in Fig. 3.

Electrical wire-resistance strain gages were mounted at each of three sections. Vertical dial gages were placed under the box beams at the first and at the second sections gaged, which are 28.22 inches and 17.72 inches from the south support, respectively.

A typical test setup is shown in Figs. 3 and 4.[9]

4. TEST RESULTS

4.1 Presentation of Test Results

4.1.1 Experimental Moment Percentages

In this study, the moment percentage for a specific beam is defined as the bending moment in that beam divided by the sum of the bending moments in all of the beams at a given section. The experimental bending moments were calculated from stress blocks obtained from the measured strains in each beam.

The exterior beams were analyzed as acting compositely with the slab, curbs, and parapets whenever they were present. Thus, the bending moments contributed by the individual slab, curbs, and parapets were taken into account in the calculations of the experimental moment percentages for all of the beams. Through the use of a GE 225 digital computer with a rather complicated, but comprehensive program, these calculations were performed on the same day of the test. The synthetic description of this computer program can be found in Ref. 9.

The experimental moment percentages for all beams with the load on lanes 1, 2, and 3 are presented in table form. Tables 3, 4, 5, 6, 15, and 16 contain experimental moment percentages at Section 1 (nominal maximum moment) for the models with four 4 ft. x 39 in. (4 x 39) box beams; Tables 7, 8, 9, and 10 present similar values for models with four 4 x 30 box beams; and Tables 11, 12, 13, and 14 correspond to the bridge models with four 3 x 42 box beams. Furthermore, the results for the bridge models A1, B15, and B16 are presented in Tables 2, 17, and 18.

4.1.2 Deflection Percentages and Rotation Percentages

Section 2 (nominal third point of the span), in addition to Section 1, was gaged in order to measure cross-sectional deflections and beam rotations. As deflections were measured at the east and west faces of each beam, the average of these two values was used to represent the mid-width deflection of each beam.

The deflection percentage of a particular beam is defined as the deflection of that beam divided by the sum of the deflections of all of the beams at a given section. The rotation percentage of a particular beam is the rotation of that beam divided by the sum of the absolute values of the rotations of all of the beams at a given section.

Values of deflection percentages and rotation percentages at Section 1 in the model tests are listed in Tables 2 through 18.

4.2 Analysis of Test Results

4.2.1 Cross-Sectional Strain Distribution

The experimental strains from two model tests are plotted along the faces of an exterior beam in Figs. 4 and 5. In most instances, a linear relationship existed in the slab and box beams. In the glued model A1, in which the curbs and parapets were cemented together, this linear variation extended with full interaction into the curbs, and with approximately 60% interaction into the parapets. In the bolted models, in which curbs and parapet pieces were bolted to the slab and to the curb, respectively, the measured strains at the top surface of the parapets were only 20% to 30% of the strains that would correspond to full linear strain variation. A possible reason for this deviation is mainly that the connection between curbs and parapets was not strong enough to develop full composite action. Another cause is that the strain gages at the top surface of the parapets were not in vertical alignment with those in the box beams and curbs. However, the experimental strain distribution obtained from model tests demonstrated that full composite action was developed in the interior beam-slab units, and in the exterior beams between the beam-slab unit and the curb.

Several strain readings were taken to investigate the strain distribution in the top surface of the slab. The longitudinal slab strains, although found to be in the same vertical linear variation with the strains in the corresponding beams, were found to depart somewhat from the linear variation in the transverse direction.

4.2.2 Location of Neutral Axes

The computation of the neutral axis location was based on linear strain distribution. The distances, in inches, from the top fiber of the box beam to the neutral axis on the east and west faces of the beams in models A1 and B1 are presented in Table 19. Based on these values, the locations of neutral axes were plotted in Figs. 6 and 7. The rotations of the neutral axes with respect to horizontal axes were also calculated and tabulated in these figures.

The test results shown indicate that the neutral axes in the exterior beams were inclined for the load on any lane, while appreciable inclination of interior beam neutral axes occurred only when the load was on the side of the bridge opposite to the beam under consideration. The inclination of the neutral axes, which was less than 15° in all cases, did not produce an appreciable effect in the calculation of the bending moment M_x, if θ was assumed equal to 0° in Eqs. 8 and 9.

4.2.3 Correlation Between Rotation and Moment Percentages

From the test results presented, it can be seen that the transverse rotation of the beams was very small, and that the range of absolute rotations under vehicular load varied from 0 to 800 millionths of a radian, depending on the rigidity of the cross-section of the bridge.

In order to study the correlation between rotations of the beams and bending moment distribution, four typical plots of λ (the ratio of experimental moment percentage to deflection percentage) against rotation percentages are shown in Figs. 20, 21, 22, and 23. Each plot was chosen, from the test results of seventeen models, to represent a typical case. Figures 20 through 23 show results of model B1 for Case (0,0,0); model B6 for Case (0,0,1); model B11 for Case (1,1,0) and model A1 for Case (1,1,1), respectively.

A common characteristic was observed. In each figure, λ - rotation percentage relationships were plotted for both exterior and interior beams with the truck on the five different loading lanes. These figures indicate that the values of λ were insensitive to rotation of the beams when the load was on the same half of the roadway. The variation of λ increased considerably when the load was on the other half of the roadway. It was also observed that the rotation percentages decreased appreciably when the load was moved from lane 4 to lane 5.

As a consequence of these observations, it is believed that the rotations of the beam cross-sections do not bear any primary relationship with the bending moment distributions. In other words, no simple correlation was found between moment percentages and rotation percentages. On the other hand, it is believed that the rotations of the beams should play a more important role in torsional moment distribution. No attempt has been made to establish a correlation between torsional moment distribution and rotation percentages.

4.2.4 Correlation Between Moment and Deflection Percentages

The experimental moment percentages in all beams at test Section 1 are compared with the deflection percentages in Figs. 8 through 19. Four model test results were chosen to represent the comparisons in four typical cases, as mentioned in Section 4.2.3. In each case, comparisons are made in three figures corresponding to the load in lanes 1, 2, and 3, respectively.

Figures 8, 9, and 10 show a typical comparison of the experimental moment percentages and deflection percentages for Case (0,0,0). It can be easily seen that the ratios of moment percentages to deflection percentages are very close to a value of one, with a maximum relative deviation of 10.5% in interior beams and of 7.1% in exterior beams. In addition, these figures show that the exterior beams had slightly smaller moment percentages than deflection percentages.

Using the data from model B6, the effect of midspan and end diaphragms on the moment distributions and deflection distributions is illustrated in Figs. 11, 12, and 13. It can be observed that the experimental moment percentages in the exterior beams are slightly larger than the deflection percentages when the load is placed on lane 1 or lane 2. Furthermore, Fig. 13 shows that moment percentages are almost identical to deflection percentages when the load is on lane 3.

In addition, the effect due to diaphragms is obtained by a comparison of the data from models B1 and B2. The most noticeable consequence of adding diaphragms is that the load is distributed more uniformly across the bridge. However, the corresponding changes introduced in the moment percentages and in the deflection percentages of exterior beams are essentially the same. In other words, the presence of diaphragms did not produce any significant change on the correlation between bending moment percentages and deflection percentages.

For the bridges with curbs and parapets, Case (1,1,0) and Case (1,1,1), the comparisons of experimental moment and deflection percentages are given in Figs. 14 through 19. In these two cases, there is an appreciable discrepancy between the bending moment distributions and deflection distributions. In general, for exterior beams, the moment percentages are substantially higher than the corresponding deflection percentages, but the opposite situation occurs for interior beams. The values of ratios of moment percentages to deflection percentages range between 0.91 to 1.27 for exterior beams, and between 0.65 to 0.91 for interior beams. This discrepancy is especially obvious when the load is on lane 1. Therefore, in these two cases, the deflection distribution cannot be used as a direct indication of the bending moment distribution. As a result, the difference in the flexural stiffness of the exterior and interior beam-slab units should be taken into consideration.

4.2.5 Effects of Vehicular Loading

The close agreement between moment and deflection percentages in the bridges without curbs and parapets indicates that it may be reasonable to conclude that the moment-deflection relationship is quite similar for all of the beams when the bridge is subjected to vehicular loading. Therefore, there is no need to make a correction to take into account the effects due to each individual concentrated wheel load, as suggested in Ref. 4.

4.2.6 Effects Due to Other Parameters

Comparison of test results from model B4 with those from models B13 and B14, shows the effect of different thickness of slab on the correlation between moment and deflection percentages. Although a thicker slab produced a somewhat more uniform lateral load distribution than a thinner slab, the ratios of moment percentages to deflection percentages were nearly identical in these three cases. Hence, the correlation between bending moment distributions will remain the same for the box-beam bridges with different thicknesses of slab.

In addition, Table 35 shows that the experimental moment percentages for model B15 are in close agreement with the deflection percentages. The lateral load distributions obtained are very close to those in model B1. The same agreement may be found in Table 36 for the bridge with seven smaller identical (3 x 24) box beams. All of the above observations indicate that the number, size, and spacing of box beams do not significantly affect the correlation between moment percentages and deflection percentages.

5. PROPOSED METHOD FOR ESTIMATING BENDING MOMENT

5.1 Development of the Proposed Method

As discussed in Chapter 2, the elastic structural behavior of box-beam bridges under vehicular loads is extremely complicated, and no exact method of analysis has been reached. The analysis is further complicated by the presence of curbs, parapets, and diaphragms. Therefore, drastic simplifications and assumptions are essential in a reasonably approximate theoretical solution.

The assumptions made in Chapter 2 led to a simplified correlation between distributions of longitudinal bending moments and of cross-sectional deflections, as shown in Eqs. 11 and 12. It is apparent that the computations for I_{eq}, equivalent moments of inertia of individual beam-slab units, are still rather lengthy and cumbersome. In order to simplify the practical application, one further assumption should be made: the neutral axes in box beams are assumed to be horizontal and passing through the centroid of each beam-slab unit.

Based on this assumption, I_{eq}, shown in Eq. 8, can be simplified to I_{xx}. This results in a much simpler correlation, which is given as follows:

$$(M.P.)_i = \frac{(I_{xx})_i \ (\delta_y)_i}{\sum_{i=1}^{m} (I_{xx})_i \ (\delta_y)_i} \tag{13}$$

By dividing $(I_{xx})_i$ by I_o and $(\delta_y)_i$ by $\Sigma\ (\delta_y)_i$, this equation can be non-dimensionalized to

$$(M.P.)_i = \frac{(F.M.I.)_i \ (D.P.)_i}{\sum_{i=1}^{m} (F.M.I.)_i \ (D.P.)_i} \tag{14}$$

where I_o is the moment of inertia of a reference box beam with respect to its horizontal centroidal axis,

F.M.I. is the factor of moment of inertia, defined as the ratio of I_{xx}/I_o, and

D.P. is the deflection percentage of an individual beam-slab unit.

The only undefined variable in computing I_{xx} is the individual slab width. Although a slab width varies appreciably when the load is on different lanes, its effect on the magnitude of I_{xx} and on F.M.I. was found to be small. (See Figs. 24 and 25.)

Therefore, the center-to-center spacing of box beams is used as the individual slab width for interior beams, and edge-of-slab to the first mid-spacing as the individual slab width for exterior beams. According to this simplification, the values of the so-called "Hypothetic Factor of Moment of Inertia" for the bridges with three different sizes of box beams were calculated and presented in Table 20. In each case, the hypothetic F.M.I. were computed based on three different thicknesses of slab and four different percentages of effectiveness of parapets: 0%, 30%, 60%, and 100%.

To study the validity of the hypothetic F.M.I., a comparison of experimental and hypothetic values was made and is presented in Table 21. The experimental F.M.I. values were based on the experimental individual slab widths.

In Table 21, it is seen that the values of hypothetic F.M.I. are nearly equal to the corresponding values of average experimental F.M.I. for exterior beams, and approximately 4 - 10% smaller in interior beams. Therefore, a complete set of suggested values of Factor of Moment of Inertia is presented in Table 22. For convenience, these tabulated values are also presented in Figs. 26 through 28. In these figures, the required values of F.M.I. can be read directly or by interpolation for different combinations of slab thickness and effectiveness of parapets.

The moment percentages based on the experimental F.M.I. are tabulated in Tables 2 through 18 under the title of "computed moment percentages". The influence of using suggested F.M.I. can be found by comparing these computed moment percentages with estimated moment percentages based on the following proposed method:

Step 1. Compute the deflection percentages (D.P.) for each box beam by using the cross-sectional deflections (δ_y), which would be obtained by direct measurements.

Step 2. Adopt a value for the percentages of effectiveness of parapets in accordance with the nature of the connection, and then determine the values of Factor of Moment of Inertia for all beams by the use of the provided charts. If the thickness is not available in the charts, the required values can be found by interpolation.

Step 3. Compute the coefficients of moment of inertia (C.M.I.) for all beams by dividing the F.M.I. of each beam by the summation of F.M.I.'s of all of the beams.

Step 4. Calculate the estimated moment percentages (E.M.P.) using the following formula.

$$(\text{E.M.P.})_i = \frac{(\text{C.M.I.})_i\ (\text{D.P.})_i}{\sum_{i=1}^{m} (\text{C.M.I.})_i\ (\text{D.P.})_i} \qquad (15)$$

Step 5. Finally, determine the estimated longitudinal bending moments by multiplying the total bending moments at the section concerned by the E.M.P.'s.

5.2 Illustrated Example

An example to illustrate the proposed method is presented as follows:

The problem is to find the moment percentages at Section 1 in Bridge Model B4 when the load is on lane 1 by using the following information:

1. The cross-sectional deflections (in 10^{-5} in.) are 489 for beam 1; 379 for beam 2; 229 for beam 3; and 120 for beam 4.
2. The bridge has four 4 x 39 box beams, slab 8 in. in thickness, curbs, parapets, and diaphragms.

Solution:

Step 1. Deflection Percentages (D.P.)

$$(D.P.)_1 = \frac{489}{(489 + 379 + 229 + 120)}(100) = 40.18$$

Similarly

$$(D.P.)_2 = 31.13$$

$$(D.P.)_3 = 18.82$$

$$(D.P.)_4 = 9.86$$

Step 2.

Thirty percent of parapet effectiveness can be considered as contributing to the flexural stiffness of this bridge, based on Fig. 5.

The suggested values of F.M.I. are taken from the charts in Fig. 26.

$$(F.M.I.)_{1,4} = 3.74$$

$$(F.M.I.)_{2,3} = 2.75$$

Step 3. Coefficients of Moment of Inertia:

$$(C.M.I.)_{1,4} = \frac{3.74}{(3.74 + 2.75)\ (2)} = 1.12$$

$$(C.M.I.)_{2,3} = \frac{2.75}{(3.74 + 2.75)\ (2)} = 0.88$$

Step 4. Estimated Moment Percentages from Eq. 15

$$(E.M.P.)_1 = \frac{(1.12)\ (40.18)}{(1.12)(40.18 + 9.86) + (0.88)(31.14 + 18.82)} = 44.96$$

Similarly

$$(E.M.P.)_2 = 27.43$$

$$(E.M.P.)_3 = 16.58$$

$$(E.M.P.)_4 = 11.03$$

5.3 Comparisons of Experimental and Estimated Moment Percentages

Using the proposed method, values of estimated moment percentages were calculated and compared with experimental moment percentages for the Berwick Bridge and eight bridge models. The results are presented in Tables 23 through 31. As mentioned in Section 4.2.1, a 60% effectiveness of the parapets was assumed in model A1 and the Berwick Bridge, and a 30% effectiveness of the parapets in models B3, B4, B7, B8, B12, B13, and B14.

Satisfactory agreement was found in all cases between the experimental and estimated moment percentages. In particular, the differences were minimal for all models when the load was on lane 3.

For the bridge models with curbs, parapets, and with or without diaphragms, the maximum difference in the comparison is within 3% of the total resisting bending moment at Section 1. In most instances, this occurred in beam 1 when the load was on lane 1. The reason is possibly due to the fact that the assumed percentages of effectiveness of the parapets were not entirely valid when the load was on lane 1. On the other hand, virtually identical results were obtained when the load was on lane 3. This can be explained by the fact that the neutral axes in the box beams with the load on lane 3 are almost horizontal, and thus, the assumption ($I_{eq} = I_{xx}$ or $\theta = 0^\circ$) can be better satisfied.

For the bridges without curbs and parapets, the equivalent moments of inertia of individual beam-slab units are nearly equal. It is reasonable to assume that the I_{eq}'s are the same in all beam-slab units. Therefore, by Eq. 12, the estimated moment percentages can be taken as equal to the deflection percentages; and the comparison of estimated and experimental moment percentages becomes that of experimental moment percentages and deflection percentages as discussed in Section 4.2.4. For convenience, this comparison is given in Tables 32 through 36.

The comparison for the Berwick Bridge is shown in Table 23. The differences between the experimental and the estimated moment percentages are slightly larger than in the models. However, for practical purposes, the estimated values are still acceptable. The deflections used in the Berwick Bridge were based on the crawl-speed field tests.

5.4 Validity and Limitations of the Proposed Method

Since the proposed method was developed by using the theoretical correlation between the bending moment distribution and the cross-sectional deflections, all of the assumptions made in Sections 2.2 and 5.1 should be satisfied. It may be noted that most of these assumptions and simplifications have already been discussed and evaluated in Sections 4.2 and 5.1. In this section, more attention is given to the discussion of the assumptions which are not always valid, and to the limitations of this method. This discussion can be summarized as follows:

1. The linear longitudinal slab strain distribution in the transverse direction is a simplifying assumption which produces some error in the computation of the experimental moment percentages.[9]

2. It was assumed in this method that the bridge is homogeneous. Actually, the modulus of elasticity for the cast-in-place slab, curbs, parapets, and diaphragms is lower than that of the box beams. This again, introduces certain errors in estimating bending moments by the proposed method.

3. The neutral axes were assumed to be horizontal and passing through the centroid of each beam-slab unit. This condition was found to exist in all model tests,

only when the load was on lane 3.

4. This method can be used to estimate the longitudinal bending moments in box-beam bridges within the elastic range only. The transverse bending moments and inelastic structural behavior are not to be determined by this method.

5. The charts provided in Figs. 26, 27, and 28 are applicable to bridges constructed according to bridge standards similar to those of the Pennsylvania Department of Highways.[a] For a bridge with different design of curb and parapet, the provided charts cannot be used. The true factors of moment of inertia should be calculated by adequate consideration of the reserve strength in curbs and parapets.

6. CONCLUSIONS

The lateral distribution of static vehicular loads in prestressed concrete box-beam bridges, within the elastic range, has been successfully estimated for eighteen different cross-sections. Within the scope of this report, the following conclusions were reached:

1. In box-beam bridges without curbs and parapets, the moment percentages were found to be essentially the same as the deflection percentages under vehicular loads. Both the theoretical analysis and the test results confirmed this conclusion.

2. The test results consistently indicated full composite action between the slab and the curb sections, and some degree of composite action between curb and parapet sections. This degree of composite action is believed to be one of the primary reasons for the difference between the distributions of longitudinal bending moments and that of cross-sectional deflections. Thus, the reserve strength contributed by curbs and parapets should be accounted for in the analysis and design.

3. Since a reasonable agreement was found in the comparison of the experimental moment percentages and the estimated moment percentages by

the proposed method, the lateral distribution of longitudinal bending moments may be estimated within acceptable accuracy using the proposed method for the bridges with curbs and parapets.

4. It appears that the presence of midspan and end diaphragms has little effect on the correlation between the distributions of longitudinal bending moments and the cross-sectional deflections.

5. The plots of the ratios of moment percentages to deflection percentages against rotation percentages indicate that there is no simple relationship between the lateral distribution of bending moments and the transverse individual rotations in box-beam bridges.

6. In a box-beam bridge under vehicular loading, the moment-deflection relationship is quite similar for all beams, regardless of vehicle location. This is due to the fact that the effects on the non-proportionality between strains and deflections is greatly reduced when multiple wheel loads are used instead of a single concentrated load.

7. The proposed method has been primarily evaluated by the test results of four-beam bridges. It is believed that further study of load distribution for three-beam and five-beam bridges might be helpful in establishing a better

understanding of the reliability of this method.

8. Every step of the proposed method can be carried out by means of a system of electronic circuits built into instrument modules. The circuits can be readily set in accordance with the bridge cross-section characteristics. It would be possible to devise a testing system in order to measure beam deflections by the use of deflectometers. The cross-sectional deflections could then be fed to a set of inter-connected instrument modules, and the moment percentages could be read directly in digital counters. Through this idea, a more efficient and more economical method can be used for both field and laboratory investigations.

7. ACKNOWLEDGMENTS

This report presents partial results of the project entitled "A Structural Model Study of Load Distribution in Highway Bridges", conducted at Fritz Engineering Laboratory of Lehigh University, Bethlehem, Pennsylvania. Dr. D. A. VanHorn is director of this research project and Chairman of the Department of Civil Engineering. Dr. L. S. Beedle is Director of the Laboratory. This project was sponsored by the National Science Foundation.

The writers wish to thank Mr. Felix Barda for his assistance in the testing portion of this investigation, and Miss Sharon Gubich for her graphic arts work.

Special thanks are due to Mrs. Carol Kostenbader for her patience, willingness, and ability in typing this manuscript.

8. TABLES

Table 1 Models Tested

Model No.	Number of Beams	Size of Beams	Slab Thick. (in.)	Curbs*	Parapets*	Dia-phragms*	File Comp. Output
A1	4	4x39	0.5	1	1	1	I23
B1	4	4x39	0.5	0	0	0	a
B2	4	4x39	0.5	0	0	1	n
B3	4	4x39	0.5	1	1	0	m
B4	4	4x39	0.5	1	1	1	e
B5	4	4x30	0.5	0	0	0	k
B6	4	4x30	0.5	0	0	1	l
B7	4	4x30	0.5	1	1	0	j
B8	4	4x30	0.5	1	1	1	i
B9	4	3x42	0.5	0	0	0	o
B10	4	3x42	0.5	0	0	1	r
B11	4	3x42	0.5	1	1	0	p
B12	4	3x42	0.5	1	1	1	q
B13	4	4x39	0.375	1	1	1	g
B14	4	4x39	0.625	1	1	1	f
B15	4	2-3x42 2-4x30	0.5	0	0	0	s
B16	7	3x24	0.5	0	0	0	t

*Code: A zero means NO and a one means YES.

Table 2 Summary of Test Results (Model A1)

BRIDGE MODEL NUMBER A 1

LOAD POSITION 1 SECTION NUMBER 1

	BEAM 1	BEAM 2	BEAM 3	BEAM 4
EXPERIMENTAL MOMENT PERCENTAGES				
LANE 1	44,57	27,02	15,43	12,98
LANE 2	33,32	26,61	20,33	19,74
LANE 3	25,50	24,50	24,50	25,50
BEAM DEFLECTION PERCENTAGES				
LANE 1	36,20	29,62	20,59	13,59
LANE 2	29,03	29,77	23,86	17,34
LANE 3	22,74	27,26	27,26	22,74
RATIO OF MOMENT PER, / DEFLECTION PER,				
LANE 1	1,23	0,91	0,75	0,96
LANE 2	1,15	0,89	0,85	1,14
LANE 3	1,12	0,90	0,90	1,12
BEAM ROTATION PERCENTAGES				
LANE 1	-15,07	-33,42	-26,30	-25,21
LANE 2	14,15	-13,21	-38,68	-33,96
LANE 3	29,44	20,56	-20,56	-29,44
COMPUTED MOMENT PERCENTAGES				
LANE 1	42,85	24,73	17,72	14,70
LANE 2	34,26	24,45	20,67	20,63
LANE 3	26,01	23,99	23,99	26,01
MOMENT OF INERTIA IO= 2,138 IN**3				
LANE 1	4,20	2,96	3,05	3,83
LANE 2	4,07	2,83	2,99	4,10
LANE 3	4,01	3,08	3,08	4,01
COEFFICIENTS OF MOMENT OF INERTIA				
LANE 1	1,20	0,84	0,87	1,09
LANE 2	1,16	0,81	0,85	1,17
LANE 3	1,13	0,87	0,87	1,13

Table 3 Summary of Test Results (Model B1)

BRIDGE MODEL NUMBER B 1

LOAD POSITION 1 SECTION NUMBER 1

	BEAM 1	BEAM 2	BEAM 3	BEAM 4
EXPERIMENTAL MOMENT PERCENTAGES				
LANE 1	44,80	32,45	15,11	7,64
LANE 2	30,20	34,81	22,32	12,67
LANE 3	19,32	30,68	30,68	19,32
BEAM DEFLECTION PERCENTAGES				
LANE 1	44,78	30,42	16,87	7,93
LANE 2	30,92	32,99	22,87	13,22
LANE 3	20,78	29,22	29,22	20,78
RATIO OF MOMENT PER. / DEFLECTION PER.				
LANE 1	1,00	1,07	0,90	0,96
LANE 2	0,98	1,06	0,98	0,96
LANE 3	0,93	1,05	1,05	0,93
BEAM ROTATION PERCENTAGES				
LANE 1	-15,54	-39,62	-29,42	-15,42
LANE 2	19,72	-10,74	-41,55	-27,99
LANE 3	26,03	23,97	-23,97	-26,03
COMPUTED MOMENT PERCENTAGES				
LANE 1	49,48	26,59	16,50	7,43
LANE 2	30,22	33,85	23,94	12,00
LANE 3	20,33	29,67	29,67	20,33
MOMENT OF INERTIA IO= 2,106 IN**3				
LANE 1	3,06	2,42	2,71	2,59
LANE 2	2,72	2,86	2,91	2,53
LANE 3	2,67	2,77	2,77	2,67
COEFFICIENTS OF MOMENT OF INERTIA				
LANE 1	1,13	0,90	1,00	0,96
LANE 2	0,99	1,04	1,06	0,92
LANE 3	0,98	1,02	1,02	0,98

Table 4 Summary of Test Results (Model B2)

BRIDGE MODEL NUMBER B 2

LOAD POSITION 1 SECTION NUMBER 1

	BEAM 1	BEAM 2	BEAM 3	BEAM 4
EXPERIMENTAL MOMENT PERCENTAGES				
LANE 1	42,65	29,76	16,52	11,07
LANE 2	31,50	31,09	21,51	15,90
LANE 3	22,71	27,29	27,29	22,71
BEAM DEFLECTION PERCENTAGES				
LANE 1	40,90	30,74	18,68	9,68
LANE 2	30,98	30,78	22,78	15,46
LANE 3	22,55	27,45	27,45	22,55
RATIO OF MOMENT PER, / DEFLECTION PER,				
LANE 1	1,04	0,97	0,88	1,14
LANE 2	1,02	1,01	0,94	1,03
LANE 3	1,01	0,99	0,99	1,01
BEAM ROTATION PERCENTAGES				
LANE 1	-17,45	-35,98	-29,12	-17,45
LANE 2	5,45	-20,05	-48,76	-25,74
LANE 3	24,02	25,98	-25,98	-24,02
COMPUTED MOMENT PERCENTAGES				
LANE 1	44,08	28,83	17,40	9,68
LANE 2	30,65	31,11	22,84	15,40
LANE 3	22,61	27,39	27,39	22,61
MOMENT OF INERTIA I0= 2,106 IN3**				
LANE 1	2,98	2,59	2,58	2,77
LANE 2	2,69	2,75	2,73	2,71
LANE 3	2,73	2,71	2,71	2,73
COEFFICIENTS OF MOMENT OF INERTIA				
LANE 1	1,09	0,95	0,94	1,01
LANE 2	0,99	1,01	1,00	1,00
LANE 3	1,00	1,00	1,00	1,00

Table 5. Summary of Test Results (Model B3)

BRIDGE MODEL NUMBER B 3

LOAD POSITION 1 SECTION NUMBER 1

	BEAM 1	BEAM 2	BEAM 3	BEAM 4
EXPERIMENTAL MOMENT PERCENTAGES				
LANE 1	49,02	29,88	13,33	7,77
LANE 2	34,44	32,34	19,91	13,31
LANE 3	22,71	27,79	27,79	22,21
BEAM DEFLECTION PERCENTAGES				
LANE 1	42,43	33,33	17,54	6,70
LANE 2	29,81	34,65	23,51	12,04
LANE 3	19,46	30,54	30,54	19,46
RATIO OF MOMENT PER, / DEFLECTION PER,				
LANE 1	1,16	0,90	0,76	1,16
LANE 2	1,16	0,93	0,85	1,11
LANE 3	1,17	0,91	0,91	1,14
BEAM ROTATION PERCENTAGES				
LANE 1	-8,50	-39,38	-33,71	-18,41
LANE 2	25,64	-10,26	-38,80	-25,30
LANE 3	28,48	21,52	-21,52	-28,48
COMPUTED MOMENT PERCENTAGES				
LANE 1	47,93	29,05	15,65	7,36
LANE 2	33,74	31,09	21,95	13,22
LANE 3	21,60	28,40	28,40	21,60
MOMENT OF INERTIA I0= 2,106 IN3**				
LANE 1	3,81	2,94	3,01	3,71
LANE 2	3,77	2,99	3,11	3,66
LANE 3	3,67	3,08	3,08	3,67
COEFFICIENTS OF MOMENT OF INERTIA				
LANE 1	1,13	0,87	0,89	1,10
LANE 2	1,11	0,88	0,92	1,08
LANE 3	1,09	0,91	0,91	1,09

Table 6 Summary of Test Results (Model B4)

BRIDGE MODEL NUMBER B 4

LOAD POSITION 1 SECTION NUMBER 1

	BEAM 1	BEAM 2	BEAM 3	BEAM 4
EXPERIMENTAL MOMENT PERCENTAGES				
LANE 1	47,01	28,10	14,97	9,92
LANE 2	35,13	29,30	19,31	16,26
LANE 3	24,82	25,18	25,18	24,82
BEAM DEFLECTION PERCENTAGES				
LANE 1	40,18	31,14	18,82	9,86
LANE 2	30,48	31,70	22,98	14,83
LANE 3	21,46	28,54	28,54	21,46
RATIO OF MOMENT PER, / DEFLECTION PER,				
LANE 1	1,17	0,90	0,80	1,01
LANE 2	1,15	0,92	0,84	1,10
LANE 3	1,16	0,88	0,88	1,16
BEAM ROTATION PERCENTAGES				
LANE 1	-14,52	-32,10	-36,29	-17,10
LANE 2	12,91	-11,14	-53,92	-22,03
LANE 3	17,96	32,04	-32,04	-17,96
COMPUTED MOMENT PERCENTAGES				
LANE 1	45,52	27,40	16,18	10,90
LANE 2	34,72	27,47	20,98	16,83
LANE 3	24,94	25,06	25,06	24,94
MOMENT OF INERTIA IO= 2,106 IN3**				
LANE 1	3,85	2,99	2,93	3,76
LANE 2	3,76	2,86	3,02	3,75
LANE 3	3,80	2,87	2,87	3,80
COEFFICIENTS OF MOMENT OF INERTIA				
LANE 1	1,14	0,88	0,86	1,11
LANE 2	1,12	0,85	0,90	1,12
LANE 3	1,14	0,86	0,86	1,14

Table 7 Summary of Test Results (Model B5)

BRIDGE MODEL NUMBER B 5

LOAD POSITION 1 SECTION NUMBER 1

	BEAM 1	BEAM 2	BEAM 3	BEAM 4
EXPERIMENTAL MOMENT PERCENTAGES				
LANE 1	41.03	30.85	16.86	11.26
LANE 2	30.20	32.56	22.53	14.71
LANE 3	21.10	28.90	28.90	21.10
BEAM DEFLECTION PERCENTAGES				
LANE 1	40.71	31.19	18.45	9.65
LANE 2	30.70	31.37	23.21	14.72
LANE 3	21.68	28.32	28.32	21.68
RATIO OF MOMENT PER. / DEFLECTION PER.				
LANE 1	1.01	0.99	0.91	1.17
LANE 2	0.98	1.04	0.97	1.00
LANE 3	0.97	1.02	1.02	0.97
BEAM ROTATION PERCENTAGES				
LANE 1	-19.53	-35.28	-28.50	-16.69
LANE 2	11.92	-15.99	-41.19	-30.89
LANE 3	28.42	21.58	-21.58	-28.42
COMPUTED MOMENT PERCENTAGES				
LANE 1	41.00	31.14	18.11	9.75
LANE 2	29.91	32.09	24.42	13.58
LANE 3	20.82	29.18	29.18	20.82
MOMENT OF INERTIA I0= 1.123 IN**3				
LANE 1	3.07	3.04	2.99	3.08
LANE 2	2.99	3.14	3.23	2.83
LANE 3	2.93	3.14	3.14	2.93
COEFFICIENTS OF MOMENT OF INERTIA				
LANE 1	1.01	1.00	0.98	1.01
LANE 2	0.98	1.03	1.06	0.93
LANE 3	0.96	1.04	1.04	0.96

Table 8 Summary of Test Results (Model B6)

BRIDGE MODEL NUMBER B 6

LOAD POSITION 1 SECTION NUMBER 1

	BEAM 1	BEAM 2	BEAM 3	BEAM 4
EXPERIMENTAL MOMENT PERCENTAGES				
LANE 1	39,80	29,25	17,93	13,02
LANE 2	30,75	29,93	21,95	17,37
LANE 3	23,01	26,99	26,99	23,01
BEAM DEFLECTION PERCENTAGES				
LANE 1	38,52	29,97	19,95	11,56
LANE 2	30,29	29,58	23,42	16,71
LANE 3	22,89	27,11	27,11	22,89
RATIO OF MOMENT PER, / DEFLECTION PER,				
LANE 1	1,03	0,98	0,90	1,13
LANE 2	1,02	1,01	0,94	1,04
LANE 3	1,01	1,00	1,00	1,01
BEAM ROTATION PERCENTAGES				
LANE 1	-20,73	-30,24	-27,32	-21,71
LANE 2	-1,91	-19,41	-44,71	-33,97
LANE 3	22,86	27,14	-27,14	-22,86
COMPUTED MOMENT PERCENTAGES				
LANE 1	38,80	30,17	19,34	11,68
LANE 2	30,14	29,80	23,56	16,50
LANE 3	22,74	27,26	27,26	22,74
MOMENT OF INERTIA IO= 1,123 IN**3				
LANE 1	3,09	3,08	2,97	3,10
LANE 2	3,03	3,07	3,06	3,01
LANE 3	3,02	3,05	3,05	3,02
COEFFICIENTS OF MOMENT OF INERTIA				
LANE 1	1,01	1,01	0,97	1,01
LANE 2	1,00	1,01	1,01	0,99
LANE 3	0,99	1,01	1,01	0,99

Table 9 Summary of Test Results (Model B7)

BRIDGE MODEL NUMBER B 7

LOAD POSITION 1 SECTION NUMBER 1

	BEAM 1	BEAM 2	BEAM 3	BEAM 4
EXPERIMENTAL MOMENT PERCENTAGES				
LANE 1	47,90	27,60	14,29	10,21
LANE 2	34,86	29,35	19,96	15,82
LANE 3	23,72	26,28	26,28	23,72
BEAM DEFLECTION PERCENTAGES				
LANE 1	40,19	31,85	18,78	9,18
LANE 2	29,59	32,94	23,89	13,57
LANE 3	20,40	29,60	29,60	20,40
RATIO OF MOMENT PER. / DEFLECTION PER.				
LANE 1	1,19	0,87	0,76	1,11
LANE 2	1,18	0,89	0,84	1,17
LANE 3	1,16	0,89	0,89	1,16
BEAM ROTATION PERCENTAGES				
LANE 1	-11,95	-36,55	-31,18	-20,32
LANE 2	23,31	-7,52	-37,07	-32,10
LANE 3	29,13	20,87	-20,87	-29,13
COMPUTED MOMENT PERCENTAGES				
LANE 1	47,48	25,56	16,37	10,58
LANE 2	35,52	27,06	21,36	16,07
LANE 3	24,02	25,98	25,98	24,02
MOMENT OF INERTIA IO= 1,123 IN**3				
LANE 1	4,65	3,16	3,43	4,54
LANE 2	4,61	3,16	3,44	4,55
LANE 3	4,55	3,39	3,39	4,55
COEFFICIENTS OF MOMENT OF INERTIA				
LANE 1	1,18	0,80	0,87	1,15
LANE 2	1,17	0,80	0,87	1,15
LANE 3	1,15	0,85	0,85	1,15

Table 10 Summary of Test Results (Model B8)

BRIDGE MODEL NUMBER B 8

LOAD POSITION 1 SECTION NUMBER 1

	BEAM 1	BEAM 2	BEAM 3	BEAM 4
EXPERIMENTAL MOMENT PERCENTAGES				
LANE 1	46,77	25,92	14,80	12,51
LANE 2	35,04	27,55	19,11	18,30
LANE 3	26,18	23,82	23,82	26,18
BEAM DEFLECTION PERCENTAGES				
LANE 1	38,08	30,53	20,21	11,18
LANE 2	29,67	30,79	23,66	15,88
LANE 3	22,12	27,88	27,88	22,12
RATIO OF MOMENT PER. / DEFLECTION PER.				
LANE 1	1,23	0,85	0,73	1,12
LANE 2	1,18	0,89	0,81	1,15
LANE 3	1,18	0,85	0,85	1,18
BEAM ROTATION PERCENTAGES				
LANE 1	-16,58	-31,99	-28,16	-23,26
LANE 2	10,93	-13,58	-41,80	-33,69
LANE 3	24,73	25,27	-25,27	-24,73
COMPUTED MOMENT PERCENTAGES				
LANE 1	44,98	24,67	17,39	12,96
LANE 2	35,02	25,67	20,96	18,35
LANE 3	26,43	23,57	23,57	26,43
MOMENT OF INERTIA IO= 1,123 IN**3				
LANE 1	4,64	3,18	3,38	4,56
LANE 2	4,60	3,25	3,45	4,50
LANE 3	4,61	3,26	3,26	4,61
COEFFICIENTS OF MOMENT OF INERTIA				
LANE 1	1,18	0,81	0,86	1,16
LANE 2	1,16	0,82	0,87	1,14
LANE 3	1,17	0,83	0,83	1,17

Table 11 Summary of Test Results (Model B9)

BRIDGE MODEL NUMBER B 9

LOAD POSITION 1 SECTION NUMBER 1

EXPERIMENTAL MOMENT PERCENTAGES

	BEAM 1	BEAM 2	BEAM 3	BEAM 4
LANE 1	48,15	32,10	13,44	6,31
LANE 2	31,19	36,55	21,89	10,37
LANE 3	18,14	31,86	31,86	18,14

BEAM DEFLECTION PERCENTAGES

	BEAM 1	BEAM 2	BEAM 3	BEAM 4
LANE 1	46,72	32,97	15,84	4,46
LANE 2	32,02	34,31	23,12	10,55
LANE 3	19,49	30,51	30,51	19,49

RATIO OF MOMENT PER, / DEFLECTION PER,

	BEAM 1	BEAM 2	BEAM 3	BEAM 4
LANE 1	1,03	0,97	0,85	1,41
LANE 2	0,97	1,07	0,95	0,98
LANE 3	0,93	1,04	1,04	0,93

BEAM ROTATION PERCENTAGES

	BEAM 1	BEAM 2	BEAM 3	BEAM 4
LANE 1	-18,55	-35,78	-28,24	-17,43
LANE 2	16,85	-12,40	-43,18	-27,58
LANE 3	24,79	25,21	-25,21	-24,79

COMPUTED MOMENT PERCENTAGES

	BEAM 1	BEAM 2	BEAM 3	BEAM 4
LANE 1	47,94	33,26	13,92	4,88
LANE 2	30,51	35,71	23,60	10,18
LANE 3	18,29	31,71	31,71	18,29

MOMENT OF INERTIA IO= 2,057 IN**3

	BEAM 1	BEAM 2	BEAM 3	BEAM 4
LANE 1	2,83	2,78	2,43	3,02
LANE 2	2,72	2,97	2,92	2,75
LANE 3	2,70	2,99	2,99	2,70

COEFFICIENTS OF MOMENT OF INERTIA

	BEAM 1	BEAM 2	BEAM 3	BEAM 4
LANE 1	1,02	1,01	0,88	1,09
LANE 2	0,96	1,05	1,03	0,97
LANE 3	0,95	1,05	1,05	0,95

Table 12 Summary of Test Results (Model B10)

BRIDGE MODEL NUMBER B10

LOAD POSITION 1 SECTION NUMBER 1

	BEAM 1	BEAM 2	BEAM 3	BEAM 4
EXPERIMENTAL MOMENT PERCENTAGES				
LANE 1	46,25	31,10	14,93	7,72
LANE 2	33,06	32,43	20,22	14,28
LANE 3	22,03	27,97	27,97	22,03
BEAM DEFLECTION PERCENTAGES				
LANE 1	44,64	31,99	17,18	6,18
LANE 2	32,61	31,48	22,04	13,87
LANE 3	22,37	27,63	27,63	22,37
RATIO OF MOMENT PER, / DEFLECTION PER,				
LANE 1	1,04	0,97	0,87	1,25
LANE 2	1,01	1,03	0,92	1,03
LANE 3	0,98	1,01	1,01	0,98
BEAM ROTATION PERCENTAGES				
LANE 1	-22,66	-30,12	-27,44	-19,78
LANE 2	0,00	-20,22	-54,35	-25,43
LANE 3	14,97	35,03	-35,03	-14,97
COMPUTED MOMENT PERCENTAGES				
LANE 1	45,38	32,22	15,85	6,56
LANE 2	32,32	32,51	21,32	13,85
LANE 3	21,84	28,16	28,16	21,84
MOMENT OF INERTIA I0= 2,057 IN3**				
LANE 1	2,84	2,81	2,57	2,96
LANE 2	2,83	2,95	2,76	2,85
LANE 3	2,78	2,91	2,91	2,78
COEFFICIENTS OF MOMENT OF INERTIA				
LANE 1	1,01	1,01	0,92	1,06
LANE 2	0,99	1,04	0,97	1,00
LANE 3	0,98	1,02	1,02	0,98

Table 13 Summary of Test Results (Model B11)

BRIDGE MODEL NUMBER B11

LOAD POSITION 1 SECTION NUMBER 1

	BEAM 1	BEAM 2	BEAM 3	BEAM 4
EXPERIMENTAL MOMENT PERCENTAGES				
LANE 1	52,81	30,37	12,18	4,64
LANE 2	34,09	34,58	20,58	10,75
LANE 3	19,72	30,28	30,28	19,72
BEAM DEFLECTION PERCENTAGES				
LANE 1	45,12	33,61	16,18	5,09
LANE 2	30,00	35,33	24,26	10,41
LANE 3	18,22	31,78	31,78	18,22
RATIO OF MOMENT PER, / DEFLECTION PER,				
LANE 1	1,17	0,90	0,75	0,91
LANE 2	1,14	0,98	0,85	1,03
LANE 3	1,08	0,95	0,95	1,08
BEAM ROTATION PERCENTAGES				
LANE 1	-10,50	-37,27	-33,20	-19,03
LANE 2	24,96	-7,62	-41,04	-26,38
LANE 3	26,13	23,87	-23,87	-26,13
COMPUTED MOMENT PERCENTAGES				
LANE 1	52,61	27,83	13,75	5,81
LANE 2	34,32	31,69	22,48	11,51
LANE 3	20,39	29,61	29,61	20,39
MOMENT OF INERTIA			I0=	2,057 IN**3
LANE 1	4,05	2,87	2,95	3,96
LANE 2	3,98	3,12	3,22	3,85
LANE 3	3,88	3,23	3,23	3,88
COEFFICIENTS OF MOMENT OF INERTIA				
LANE 1	1,17	0,83	0,85	1,15
LANE 2	1,12	0,88	0,91	1,09
LANE 3	1,09	0,91	0,91	1,09

Table 14 Summary of Test Results (Model B12)

BRIDGE MODEL NUMBER B12

LOAD POSITION 1 SECTION NUMBER 1

	BEAM 1	BEAM 2	BEAM 3	BEAM 4
EXPERIMENTAL MOMENT PERCENTAGES				
LANE 1	50,80	28,76	13,18	7,26
LANE 2	36,70	30,43	18,18	14,69
LANE 3	24,32	25,68	25,68	24,32
BEAM DEFLECTION PERCENTAGES				
LANE 1	43,45	32,40	17,01	7,14
LANE 2	31,59	32,67	22,03	13,72
LANE 3	21,48	28,52	28,52	21,48
RATIO OF MOMENT PER. / DEFLECTION PER.				
LANE 1	1,17	0,89	0,77	1,02
LANE 2	1,16	0,93	0,83	1,07
LANE 3	1,13	0,90	0,90	1,13
BEAM ROTATION PERCENTAGES				
LANE 1	-18,02	-32,98	-29,37	-19,63
LANE 2	8,90	-14,08	-57,76	-19,25
LANE 3	17,84	32,16	-32,16	-17,84
COMPUTED MOMENT PERCENTAGES				
LANE 1	50,67	27,25	13,76	8,31
LANE 2	36,07	29,28	19,28	15,36
LANE 3	24,24	25,76	25,76	24,24
MOMENT OF INERTIA IO= 2,057 IN3**				
LANE 1	4,01	2,89	2,78	4,00
LANE 2	3,99	3,13	3,06	3,91
LANE 3	3,92	3,14	3,14	3,92
COEFFICIENTS OF MOMENT OF INERTIA				
LANE 1	1,17	0,85	0,81	1,17
LANE 2	1,13	0,89	0,87	1,1[illegible]
LANE 3	1,11	0,89	0,89	1,11

Table 15 Summary of Test Results (Model B13)

BRIDGE MODEL NUMBER B13

LOAD POSITION 1 SECTION NUMBER 1

	BEAM 1	BEAM 2	BEAM 3	BEAM 4
EXPERIMENTAL MOMENT PERCENTAGES				
LANE 1	49,16	28,46	13,80	8,58
LANE 2	34,58	31,15	19,38	14,89
LANE 3	23,94	26,06	26,06	23,94
BEAM DEFLECTION PERCENTAGES				
LANE 1	42,85	32,10	17,87	7,19
LANE 2	29,97	32,77	22,75	14,51
LANE 3	20,90	29,10	29,10	20,90
RATIO OF MOMENT PER. / DEFLECTION PER.				
LANE 1	1,15	0,89	0,77	1,19
LANE 2	1,15	0,95	0,85	1,03
LANE 3	1,15	0,90	0,90	1,15
BEAM ROTATION PERCENTAGES				
LANE 1	-11,58	-37,95	-34,75	-15,71
LANE 2	19,08	-15,35	-44,96	-20,61
LANE 3	17,14	32,86	-32,86	-17,14
COMPUTED MOMENT PERCENTAGES				
LANE 1	49,67	26,72	15,98	7,63
LANE 2	34,36	28,75	20,97	15,92
LANE 3	24,10	25,90	25,90	24,10
MOMENT OF INERTIA IO= 2,100 IN**3				
LANE 1	3,52	2,53	2,71	3,22
LANE 2	3,43	2,62	2,75	3,28
LANE 3	3,38	2,61	2,61	3,38
COEFFICIENTS OF MOMENT OF INERTIA				
LANE 1	1,17	0,84	0,91	1,07
LANE 2	1,13	0,87	0,91	1,09
LANE 3	1,13	0,87	0,87	1,13

Table 16   Summary of Test Results (Model B14)

BRIDGE MODEL NUMBER   B14

LOAD POSITION 1   SECTION NUMBER 1

	BEAM 1	BEAM 2	BEAM 3	BEAM 4
EXPERIMENTAL MOMENT PERCENTAGES				
LANE 1	47,35	27,97	14,65	10,03
LANE 2	35,59	28,89	19,38	18,14
LANE 3	24,52	25,48	25,48	24,52
BEAM DEFLECTION PERCENTAGES				
LANE 1	40,84	31,11	18,89	9,16
LANE 2	30,87	30,78	23,20	15,15
LANE 3	22,05	27,95	27,95	22,05
RATIO OF MOMENT PER. / DEFLECTION PER.				
LANE 1	1,16	0,90	0,78	1,09
LANE 2	1,15	0,94	0,84	1,20
LANE 3	1,11	0,91	0,91	1,11
BEAM ROTATION PERCENTAGES				
LANE 1	-16,53	-30,11	-32,24	-21,11
LANE 2	4,97	-11,18	-56,83	-27,02
LANE 3	18,93	31,07	-31,07	-18,93
COMPUTED MOMENT PERCENTAGES				
LANE 1	46,35	26,67	17,28	9,70
LANE 2	34,49	27,95	21,34	16,22
LANE 3	24,32	25,68	25,68	24,32
MOMENT OF INERTIA I0= 2,106 IN3**				
LANE 1	4,26	3,22	3,43	3,97
LANE 2	4,18	3,40	3,44	4,00
LANE 3	4,08	3,40	3,40	4,08
COEFFICIENTS OF MOMENT OF INERTIA				
LANE 1	1,14	0,86	0,92	1,07
LANE 2	1,11	0,90	0,92	1,07
LANE 3	1,09	0,91	0,91	1,09

Table 17 Summary of Test Results (Model B15)

BRIDGE MODEL NUMBER B15

LOAD POSITION 1 SECTION NUMBER 1

	BEAM 1	BEAM 2	BEAM 3	BEAM 4
EXPERIMENTAL MOMENT PERCENTAGES				
LANE 1	44,95	32,16	14,71	8,16
LANE 2	29,67	34,98	23,26	12,10
LANE 3	18,70	31,30	31,30	18,70
BEAM DEFLECTION PERCENTAGES				
LANE 1	43,57	32,31	17,37	6,74
LANE 2	30,77	33,48	23,50	12,25
LANE 3	19,97	30,03	30,03	19,97
RATIO OF MOMENT PER, / DEFLECTION PER,				
LANE 1	1,03	1,00	0,85	1,21
LANE 2	0,96	1,04	0,99	0,99
LANE 3	0,94	1,04	1,04	0,94
BEAM ROTATION PERCENTAGES				
LANE 1	-15,71	-37,40	-28,14	-18,76
LANE 2	18,95	-10,54	-41,68	-28,83
LANE 3	26,16	23,84	-23,84	-26,16
COMPUTED MOMENT PERCENTAGES				
LANE 1	44,60	31,71	16,13	7,55
LANE 2	29,90	33,88	24,38	11,83
LANE 3	19,22	30,78	30,78	19,22
MOMENT OF INERTIA IO= 2,057 IN**3				
LANE 1	2,77	2,66	2,51	3,03
LANE 2	2,74	2,86	2,93	2,73
LANE 3	2,72	2,90	2,90	2,72
COEFFICIENTS OF MOMENT OF INERTIA				
LANE 1	1,01	0,97	0,92	1,11
LANE 2	0,97	1,02	1,04	0,97
LANE 3	0,97	1,03	1,03	0,97

Table 18 Summary of Test Results (Model B16)

BRIDGE MODEL NUMBER B16

LOAD POSITION 1 SECTION NUMBER 1

	BEAM 1	BEAM 2	BEAM 3	BEAM 4	BEAM 5	BEAM 6	BEAM 7
EXPERIMENTAL MOMENT PERCENTAGES							
LANE 1	25.85	21.59	16.57	12.69	8.83	7.57	6.90
LANE 2	17.73	18.27	17.24	15.07	11.94	10.31	9.45
LANE 3	12.65	14.03	15.31	16.02	15.31	14.03	12.65
BEAM DEFLECTION PERCENTAGES							
LANE 1	23.50	19.84	17.31	13.43	10.85	8.28	6.78
LANE 2	17.64	17.13	17.10	14.92	13.10	10.69	9.42
LANE 3	12.94	13.75	15.62	15.43	15.62	13.71	12.94
RATIO OF MOMENT PER. / DEFLECTION PER.							
LANE 1	1.10	1.09	0.96	0.94	0.81	0.91	1.02
LANE 2	1.01	1.07	1.01	1.01	0.91	0.96	1.00
LANE 3	0.98	1.02	0.98	1.04	0.98	1.02	0.98
BEAM ROTATION PERCENTAGES							
LANE 1	-10.21	-16.77	-19.80	-16.95	-12.80	-10.22	-7.25
LANE 2	-0.78	-3.36	-15.14	-25.29	-22.17	-20.64	-12.41
LANE 3	17.10	20.46	11.86	1.15	-11.86	-20.46	-17.10
COMPUTED MOMENT PERCENTAGES							
LANE 1	24.74	22.73	16.44	12.54	8.61	7.70	7.23
LANE 2	18.37	17.72	16.56	15.15	11.54	10.46	9.91
LANE 3	13.55	14.30	14.40	15.55	14.40	14.26	13.55
MOMENT OF INERTIA I0= 0.501 IN3**							
LANE 1	3.28	3.57	2.96	2.91	2.47	2.90	3.32
LANE 2	3.23	3.21	3.06	3.15	2.73	3.04	3.26
LANE 3	3.20	3.19	2.82	3.08	2.82	3.18	3.20
COEFFICIENTS OF MOMENT OF INERTIA							
LANE 1	1.07	1.17	0.97	0.95	0.81	0.95	1.09
LANE 2	1.04	1.04	0.99	1.02	0.88	0.98	1.05
LANE 3	1.04	1.04	0.92	1.00	0.92	1.04	1.04

Table 19 Distances (in inches) From the Top Fiber of the Beam to the Neutral Axis in the Beams

At Section 1, Bridge Model A1

Load on Lane	Beam 1 East Face	Beam 1 West Face	Beam 2 East Face	Beam 2 West Face
1	0.1931	0.1134	0.4102	0.2095
2	0.2680	0.3000	0.4384	0.3539
3	0.1823	0.4517	0.3415	0.2842
4	0.0613	0.4789	0.2765	0.4297
5	0.3745	0.5841	0.4039	0.6517

At Section 1, Bridge Model B1

Load on Lane	Beam 1 East Face	Beam 1 West Face	Beam 2 East Face	Beam 2 West Face
1	0.5279	0.3103	0.6395	0.2786
2	0.5460	0.4231	0.5224	0.3547
3	0.4670	0.5333	0.4210	0.4917
4	0.3097	0.8347	0.1725	0.6353
5	0.1348	0.8565	0.2854	0.8509

Table 20 Hypothetic Factors of Moment of Inertia (F.M.I.)

Beam Size (Prototype)	Slab Thickness (in.)	Hypothetic F.M.I.			I_o** (in^4)
		P*	Exterior Beam Use	Interior Beam Use	
4 x 39	6	0 30 60 100	2.99 3.38 3.74 4.18	2.39	2.106
	8	0 30 60 100	3.34 3.74 4.11 4.56	2.75	
	10	0 30 60 100	3.70 4.12 4.50 4.97	3.11	
4 x 39	6	0 30 60 100	3.41 4.01 4.57 5.23	2.61	1.123
	8	0 30 60 100	3.88 4.50 5.08 5.78	3.06	
	10	0 30 60 100	4.38 5.03 5.64 6.38	3.52	
4 x 39	6	0 30 60 100	3.12 3.52 3.89 4.33	2.51	2.052
	8	0 30 60 100	3.48 3.88 4.26 4.72	2.88	
	10	0 30 60 100	3.85 4.26 4.65 5.13	3.24	

Note: * P - Percentages of Effectiveness of Parapets
** I_o - Base Moment of Inertia of Box Beam

Table 21 Comparison of Experimental and Hypothetic Factors of Moment of Inertia at Section 1

(1) Brg. No.	(2) Beam No.	(3) Experimental F.M.I. Lane 1	Lane 2	Lane 3	Lane 4	Lane 5	(4) Average F.M.I.	(5) Hypoth. F.M.I.	(6) Δ* (%)
A-1	1	4.20	4.07	4.01	4.10	3.83	4.04	4.11	-1.71
	2	2.96	2.83	3.08	2.99	3.05	2.98	2.75	+7.72
B-4	1	3.84	3.74	3.78	3.73	3.74	3.76	3.74	+0.54
	2	2.99	2.86	2.87	3.02	2.93	2.93	2.75	+6.56
B-13	1	3.50	3.41	3.36	3.26	3.20	3.35	3.38	-0.89
	2	2.53	2.62	2.61	2.75	2.71	2.64	2.39	+10.05
B-14	1	4.24	4.16	4.06	3.98	3.95	4.08	4.12	-0.97
	2	3.22	3.40	3.40	3.44	3.43	3.38	3.11	+8.69
B-8	1	4.61	4.57	4.57	4.47	4.53	4.55	4.50	+1.11
	2	3.18	3.25	3.26	3.45	3.38	3.30	3.06	+7.84
B-12	1	3.99	3.97	3.90	3.89	3.98	3.95	3.88	+1.80
	2	2.89	3.13	3.14	3.06	2.78	3.00	2.88	+3.82

Note: * Δ : Difference $= \frac{(4) - (5)}{(5)} \times 100$

Table 22 Suggested Factors of Moment of Inertia (F.M.I.)

Beam Size (Prototype)	Slab Thickness (in.)	Suggested F.M.I.		
		P*	Exterior Beam Use	Interior Beam Use
4 x 39	6	0 50 100	2.99 3.59 4.18	2.57
	8	0 50 100	3.34 3.95 4.56	2.96
	10	0 50 100	3.70 4.33 4.97	3.34
4 x 39	6	0 50 100	3.41 4.32 5.23	2.80
	8	0 50 100	3.88 4.83 5.78	3.29
	10	0 50 100	4.38 5.38 6.38	3.78
4 x 39	6	0 50 100	3.12 3.73 4.33	2.70
	8	0 50 100	3.48 4.10 4.72	3.10
	10	0 50 100	3.85 4.49 5.13	3.48

Note: * P - Percentages of Effectiveness of Parapets

Table 23 Comparison of Experimental and Estimated Moment Percentages at Section 1, Northbound, Berwick Bridge

(1) Test Bridge	(2) Load on Lane	(3) Beam No.	(4) Experimental Moment Percentages	(5) Deflection Percentages	(6) Coeff. of Moment of Inertia	(7) Estimated Moment Percentages	(8) Difference (7) - (4)
Berwick Bridge (Prototype)	1	1	43.82	34.99	1.15	40.78	-3.04
		2	30.95	31.03	0.85	26.50	-4.45
		3	15.02	22.02	0.85	18.80	+3.78
		4	10.21	11.95	1.15	13.93	+3.72
	2	1	33.00	28.47	1.15	33.69	+0.69
		2	31.06	33.39	0.85	28.95	-2.11
		3	20.85	24.59	0.85	21.32	+0.47
		4	15.09	13.55	1.15	16.03	+0.94
	3	1	21.12	19.91	1.15	23.75	+2.63
		2	29.00	29.48	0.85	25.76	-2.76
		3	28.88	30.92	0.85	27.02	-1.86
		4	21.12	19.68	1.15	23.47	+2.35

Table 24 Comparison of Experimental and Estimated Moment Percentages at Section 1, Load on Position 1

(1) Bridge Model No.	(2) Load on Lane	(3) Beam No.	(4) Experimental Moment Percentages	(5) Deflection Percentages	(6) Coeff. of Moment of Inertia	(7) Estimated Moment Percentages	(8) Difference (7) - (4)
A-1	1	1	44.57	36.20	1.15	41.81	-2.76
		2	27.02	29.62	0.85	25.06	-1.96
		3	15.43	20.59	0.85	17.43	+2.00
		4	12.98	13.59	1.15	15.69	+2.71
	2	1	33.32	29.03	1.15	33.89	+0.57
		2	26.61	29.77	0.85	25.46	-1.15
		3	20.33	23.86	0.85	20.41	+0.08
		4	19.74	17.34	1.15	20.25	+0.51
	3	1	25.50	22.74	1.15	26.62	+1.12
		2	24.50	27.26	0.85	23.38	-1.12
		3	24.50	27.26	0.85	23.38	-1.12
		4	25.50	22.74	1.15	26.62	+1.12

Table 25 Comparison of Experimental and Estimated Moment Percentages at Section 1, Load on Position 1

(1) Bridge Model No.	(2) Load on Lane	(3) Beam No.	(4) Experimental Moment Percentages	(5) Deflection Percentages	(6) Coeff. of Moment of Inertia	(7) Estimated Moment Percentages	(8) Difference (7) - (4)
B-4	1	1	47.01	40.18	1.12	44.96	-2.05
		2	28.10	31.14	0.88	27.43	-0.67
		3	14.97	18.82	0.88	16.58	+1.61
		4	9.92	9.86	1.12	11.03	+1.11
	2	1	35.13	30.48	1.12	34.49	-0.64
		2	29.30	31.70	0.88	28.24	-1.06
		3	19.31	22.98	0.88	20.48	+1.17
		4	16.26	14.83	1.12	16.79	+0.53
	3	1	24.82	21.46	1.12	24.43	-0.39
		2	25.18	28.54	0.88	25.57	+0.39
		3	25.18	28.54	0.88	25.57	+0.39
		4	24.82	21.46	1.12	24.43	-0.39

Table 26 Comparison of Experimental and Estimated Moment Percentages at Section 1, Load on Position 1

(1) Bridge Model No.	(2) Load on Lane	(3) Beam No.	(4) Experimental Moment Percentages	(5) Deflection Percentages	(6) Coeff. of Moment of Inertia	(7) Estimated Moment Percentages	(8) Difference (7) - (4)
B-8	1	1	46.77	38.08	1.16	44.31	-2.46
		2	25.92	30.53	0.84	25.68	-0.24
		3	14.80	20.21	0.84	17.01	+2.21
		4	12.51	11.18	1.16	13.01	+0.50
	2	1	35.04	29.67	1.16	34.94	-0.10
		2	27.55	30.79	0.84	26.22	-1.33
		3	19.11	23.66	0.84	20.15	+1.04
		4	18.30	15.88	1.16	18.70	+0.40
	3	1	26.18	22.12	1.16	26.16	-0.02
		2	23.82	27.88	0.84	23.84	+0.02
		3	23.82	27.88	0.84	23.84	+0.02
		4	26.18	22.12	1.16	26.16	-0.02

Table 27 Comparison of Experimental and Estimated Moment Percentages at Section 1, Load on Position 1

(1) Bridge Model No.	(2) Load on Lane	(3) Beam No.	(4) Experimental Moment Percentages	(5) Deflection Percentages	(6) Coeff. of Moment of Inertia	(7) Estimated Moment Percentages	(8) Difference (7) - (4)
		1	50.80	43.45	1.12	48.62	-2.18
	1	2	28.76	32.40	0.88	28.45	-0.31
		3	13.18	17.01	0.88	14.93	+1.75
		4	7.26	7.14	1.12	7.99	+0.64
		1	36.70	31.59	1.12	35.80	-0.90
B-12	2	2	30.43	32.67	0.88	29.06	-1.37
		3	18.18	22.03	0.88	19.59	+1.41
		4	14.69	13.72	1.12	15.55	+0.86
		1	24.32	21.48	1.12	24.48	+0.16
	3	2	25.68	28.52	0.88	25.52	-0.16
		3	25.68	28.52	0.88	25.52	-0.16
		4	24.32	21.48	1.12	24.48	+0.16

Table 28 Comparison of Experimental and Estimated Moment Percentages at Section 1, Load on Position 1

(1) Bridge Model No.	(2) Load on Lane	(3) Beam No.	(4) Experimental Moment Percentages	(5) Deflection Percentages	(6) Coeff. of Moment of Inertia	(7) Estimated Moment Percentages	(8) Difference (7) - (4)
		1	49.16	42.85	1.13	48.49	-0.67
	1	2	28.46	32.10	0.87	27.86	-0.60
		3	13.80	17.87	0.87	15.51	+1.71
		4	8.58	7.19	1.13	8.14	-0.44
		1	34.58	29.97	1.13	34.42	-0.16
B-13	2	2	31.15	32.77	0.87	28.87	-2.28
		3	19.38	22.75	0.87	20.05	+0.67
		4	14.89	14.51	1.13	16.66	+1.77
		1	23.94	20.90	1.13	24.17	+0.23
	3	2	26.06	29.10	0.87	25.83	-0.23
		3	26.06	29.10	0.87	25.83	-0.23
		4	23.94	20.90	1.13	24.17	+0.23

Table 29 Comparison of Experimental and Estimated Moment Percentages at Section 1, Load on Position 1

(1) Bridge Model No.	(2) Load on Lane	(3) Beam No.	(4) Experimental Moment Percentages	(5) Deflection Percentages	(6) Coeff. of Moment of Inertia	(7) Estimated Moment Percentages	(8) Difference (7) - (4)
	1	1	47.35	40.84	1.10	44.91	-2.44
		2	27.97	31.11	0.90	28.00	+0.03
		3	14.65	18.89	0.90	17.01	+2.36
		4	10.03	9.16	1.10	10.07	+0.04
B-14	2	1	35.59	30.87	1.10	34.22	-1.37
		2	28.89	30.78	0.90	27.93	-0.96
		3	19.38	23.20	0.90	21.05	+1.67
		4	16.14	15.15	1.10	16.80	+0.64
	3	1	24.52	22.05	1.10	24.53	+0.01
		2	25.48	27.95	0.90	25.47	-0.01
		3	25.48	27.95	0.90	25.47	-0.01
		4	24.52	22.05	1.10	24.53	+0.01

Table 30 Comparison of Experimental and Estimated Moment Percentages at Section 1, Load on Position 1

(1) Bridge Model No.	(2) Load on Lane	(3) Beam No.	(4) Experimental Moment Percentages	(5) Deflection Percentages	(6) Coeff. of Moment of Inertia	(7) Estimated Moment Percentages	(8) Difference (7) - (4)
B-3	1	1	49.02	42.43	1.15	48.90	-0.12
		2	29.88	33.33	0.85	28.40	-1.44
		3	13.33	17.54	0.85	14.96	1.63
		4	7.77	6.70	1.15	7.74	-0.03
	2	1	34.44	29.81	1.15	35.15	0.71
		2	32.34	34.65	0.85	30.20	-2.14
		3	19.91	23.51	0.85	20.45	0.54
		4	13.31	12.04	1.15	14.20	0.89
	3	1	22.21	19.46	1.15	23.18	0.97
		2	27.79	30.34	0.85	26.82	-0.97
		3	27.79	30.54	0.85	26.82	-0.97
		4	22.21	19.46	1.15	23.18	0.97

Table 31 Comparison of Experimental and Estimated Moment Percentages at Section 1, Load on Position 1

(1) Bridge Model No.	(2) Load on Lane	(3) Beam No.	(4) Experimental Moment Percentages	(5) Deflection Percentages	(6) Coeff. of Moment of Inertia	(7) Estimated Moment Percentages	(8) Difference (7) - (4)
B-7	1	1	47.90	40.19	1.16	46.20	-1.70
		2	27.60	31.85	0.84	26.50	-1.10
		3	14.29	18.78	0.84	15.56	1.27
		4	10.21	9.18	1.16	11.74	1.53
	2	1	34.86	29.59	1.16	35.15	0.29
		2	29.35	32.94	0.84	28.25	-1.10
		3	19.96	23.89	0.84	20.55	0.59
		4	15.82	13.57	1.16	16.05	0.23
	3	1	23.72	20.40	1.16	24.42	0.70
		2	26.28	29.60	0.84	25.58	-0.70
		3	26.28	29.60	0.84	25.58	-0.70
		4	23.72	20.40	1.16	24.42	0.70

Table 32 Comparison of Experimental and Estimated Moment Percentages at Section 1, Load on Position 1

(1) Bridge Model No.	(2) Load on Lane	(3) Beam No.	(4) Experimental Moment Percentages	(5) Estimated Moment Percentages	(6) Difference (5) - (4)
B-2	1	1	42.65	40.90	-1.75
		2	29.76	30.74	0.98
		3	16.52	18.68	2.16
		4	11.07	9.68	-1.39
	2	1	31.50	30.98	-0.52
		2	31.09	30.78	-0.31
		3	21.51	22.78	1.27
		4	15.90	15.46	-0.44
	3	1	22.71	22.55	-0.16
		2	27.29	27.45	0.16
		3	27.29	27.45	0.16
		4	22.71	22.55	-0.16

Table 33 Comparison of Experimental and Estimated Moment Percentages at Section 1, Load on Position 1

(1) Bridge Model No.	(2) Load on Lane	(3) Beam No.	(4) Experimental Moment Percentages	(5) Estimated Moment Percentages	(6) Difference (5) - (4)
	1	1	39.80	38.52	-1.28
		2	29.25	29.97	0.72
		3	17.93	19.95	2.02
		4	13.02	11.56	-1.46
B-6	2	1	30.75	30.29	-0.46
		2	29.93	29.58	-0.35
		3	21.95	23.42	1.47
		4	17.37	16.71	-0.66
	3	1	23.01	22.89	-0.12
		2	26.99	27.11	0.12
		3	26.99	27.11	0.12
		4	23.01	22.89	-0.12

Table 34 Comparison of Experimental and Estimated Moment Percentages at Section 1, Load on Position 1

(1) Bridge Model No.	(2) Load on Lane	(3) Beam No.	(4) Experimental Moment Percentages	(5) Estimated Moment Percentages	(6) Difference (5) - (4)
B-1	1	1	44.80	44.78	-0.02
		2	32.45	30.42	-2.03
		3	15.11	16.87	1.76
		4	7.64	7.93	0.29
	2	1	30.20	30.92	0.72
		2	34.81	32.99	-1.82
		3	22.32	22.87	0.55
		4	12.67	13.22	0.55
	3	1	19.32	20.78	1.46
		2	30.68	29.22	-1.46
		3	30.68	29.22	-1.46
		4	19.32	20.78	1.46

Table 35 Comparison of Experimental and Estimated Moment Percentages at Section 1, Load on Position 1

(1) Bridge Model No.	(2) Load on Lane	(3) Beam No.	(4) Experimental Moment Percentages	(5) Estimated Moment Percentages	(6) Difference (5) - (4)
		1	44.95	43.57	-1.38
	1	2	32.16	32.31	0.15
		3	14.71	17.37	2.66
		4	8.16	6.74	-1.42
		1	29.67	30.77	1.10
B-15	2	2	34.98	33.48	-1.50
		3	23.26	23.50	0.24
		4	12.10	12.25	0.15
		1	18.70	19.97	1.27
	3	2	31.30	30.03	-1.27
		3	31.30	30.03	-1.27
		4	18.70	19.97	1.27

Table 36 Comparison of Experimental and Estimated Moment Percentages at Section 1, Load on Position 1

(1) Bridge Model No.	(2) Load on Lane	(3) Beam No.	(4) Experimental Moment Percentages	(5) Estimated Moment Percentages	(6) Difference (5) - (4)
		1	25.85	23.50	-2.35
		2	21.59	19.84	-1.75
		3	16.57	17.31	0.74
	1	4	12.69	13.43	0.74
		5	8.83	10.85	2.02
		6	7.57	8.28	0.71
		7	6.90	6.78	-0.12
		1	17.73	17.64	-0.09
		2	18.27	17.13	-1.14
		3	17.24	17.10	-0.14
B-16	2	4	15.07	14.92	-0.15
		5	11.94	13.10	1.16
		6	10.31	10.69	0.38
		7	9.45	9.42	-0.03
		1	12.65	12.94	0.29
		2	14.03	13.73	-0.30
		3	15.31	15.62	0.31
	3	4	16.02	15.43	-0.59
		5	15.31	15.62	0.31
		6	14.03	13.73	-0.30
		7	12.65	12.94	0.29

9. FIGURES

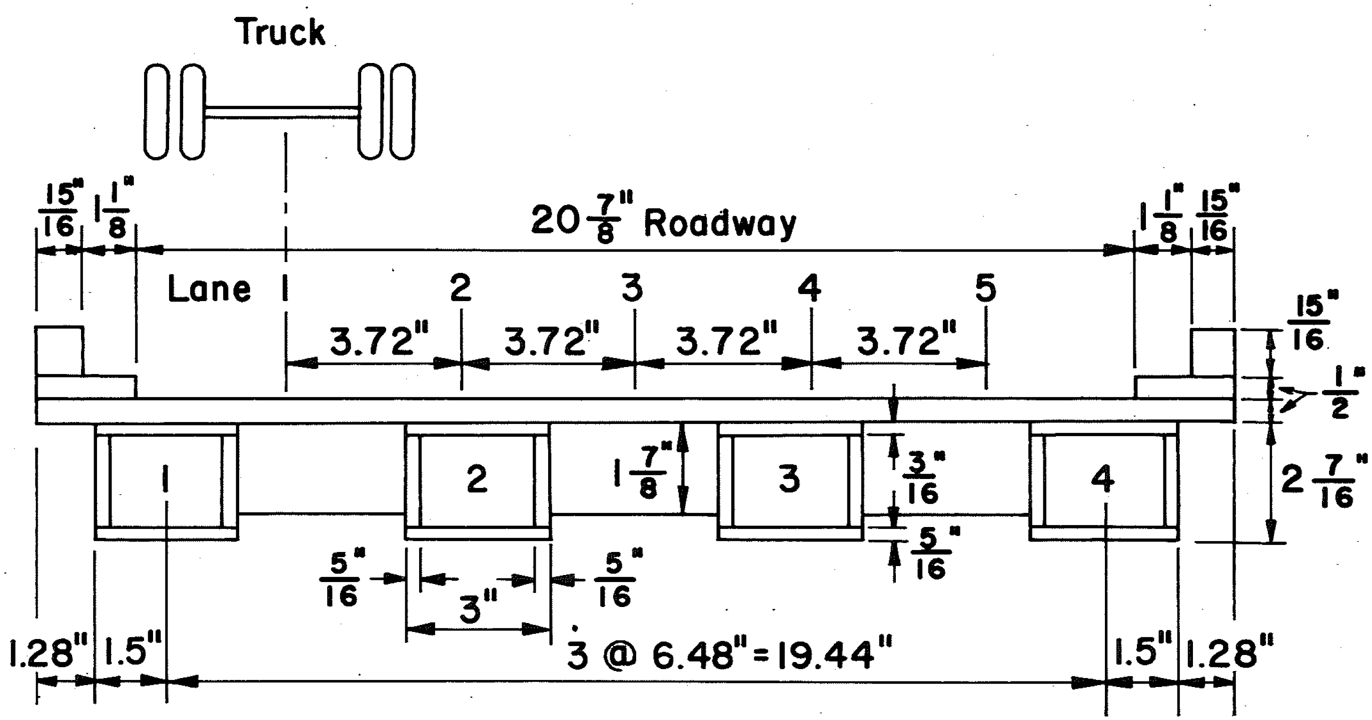

Fig. 1a Cross-Section of Model B4

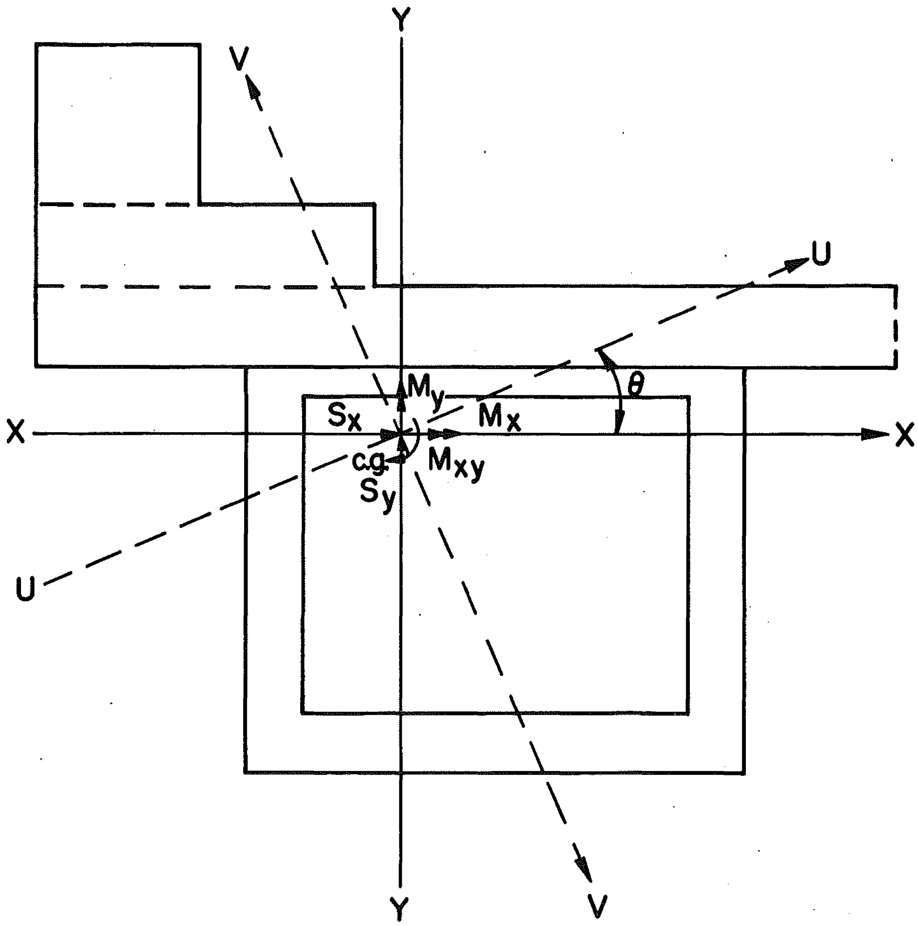

Note:

XX, YY - Horizontal and Vertical Centroidal Axes

UU, VV - Neutral Axes

θ - Angle Between Axis UU and Axis XX

Fig. 1b Beam-Slab Unit

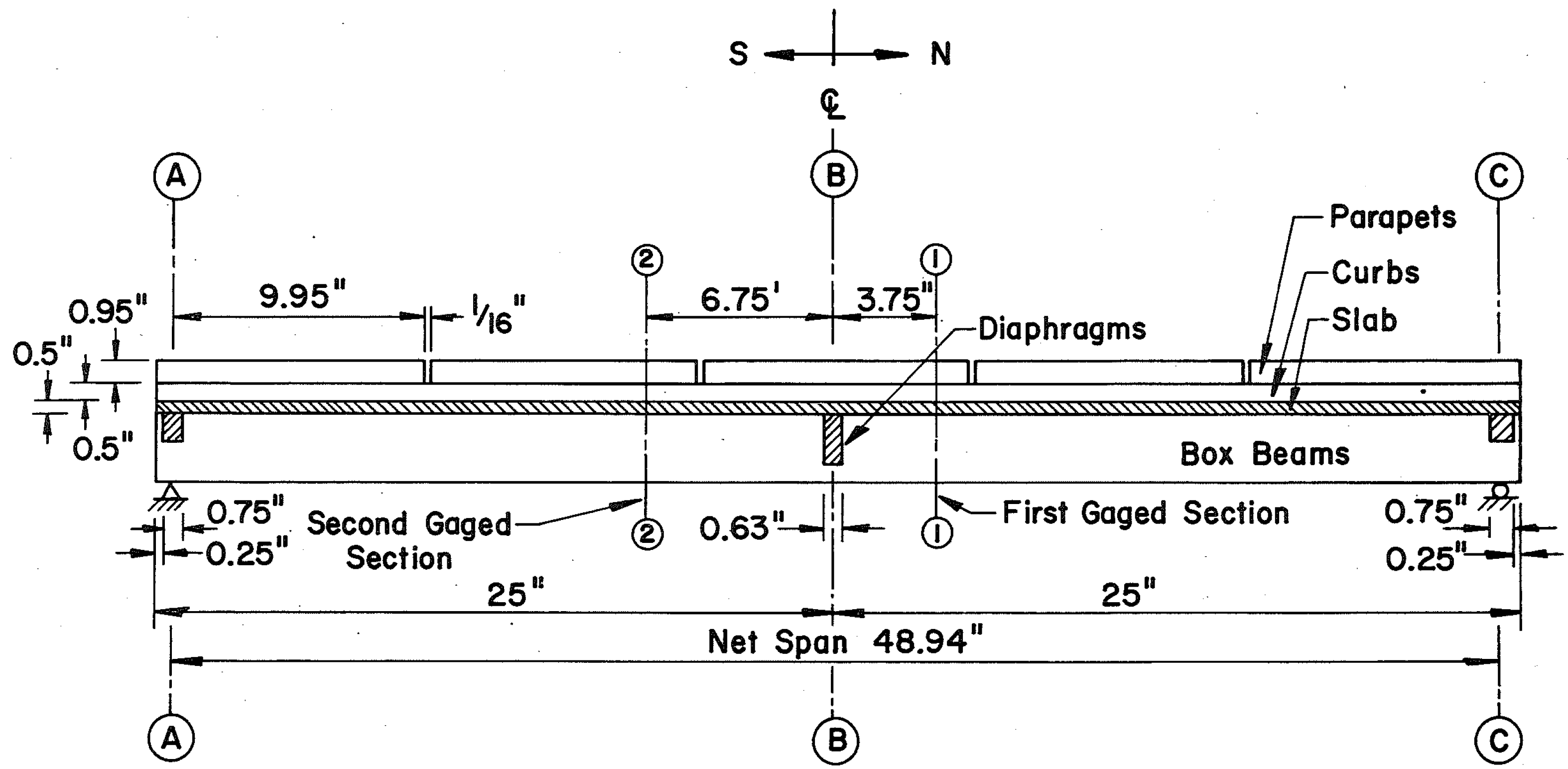

Fig. 2 Longitudinal View of a Bolted Model

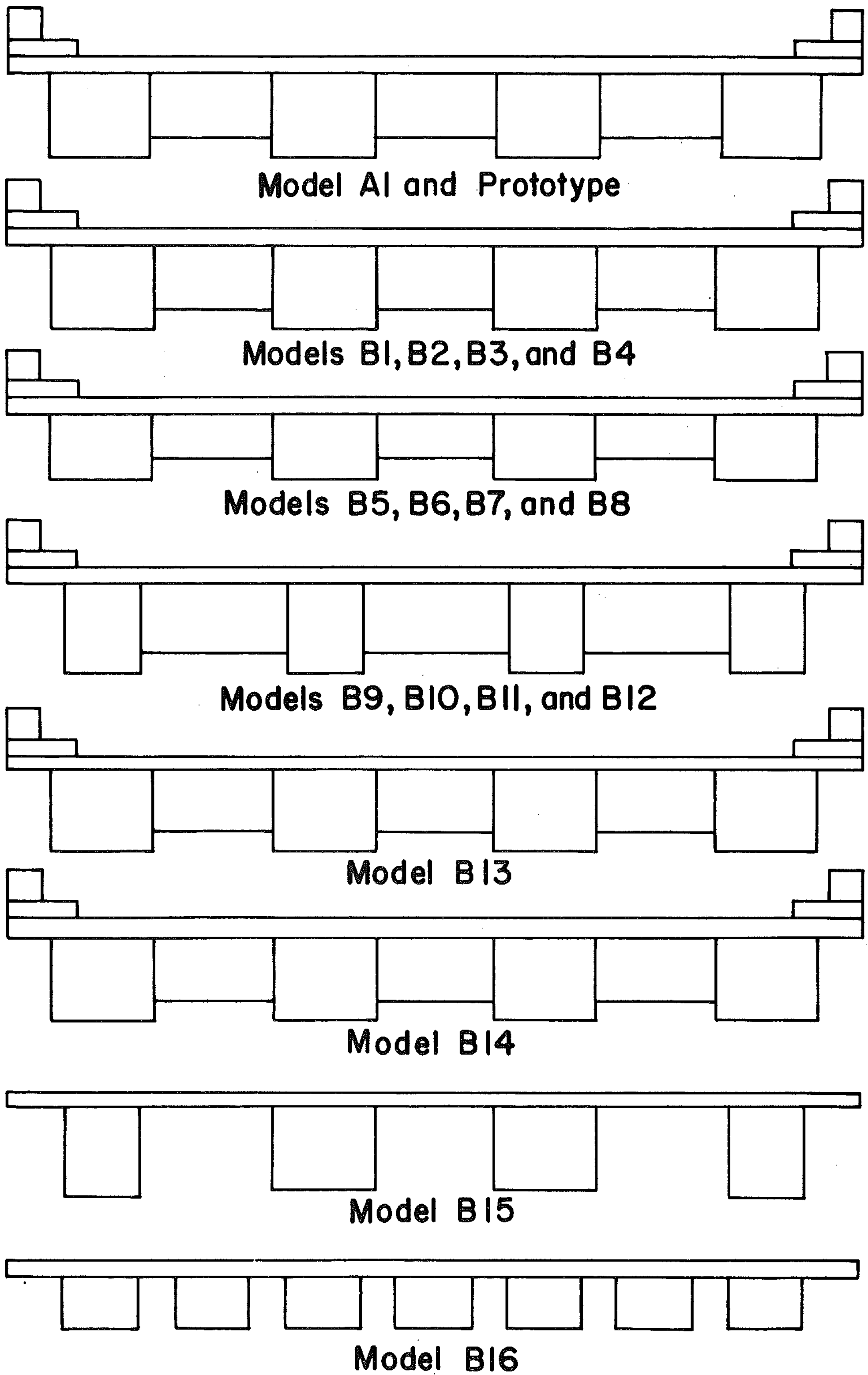

Fig. 3 Basic Cross-Sections Tested

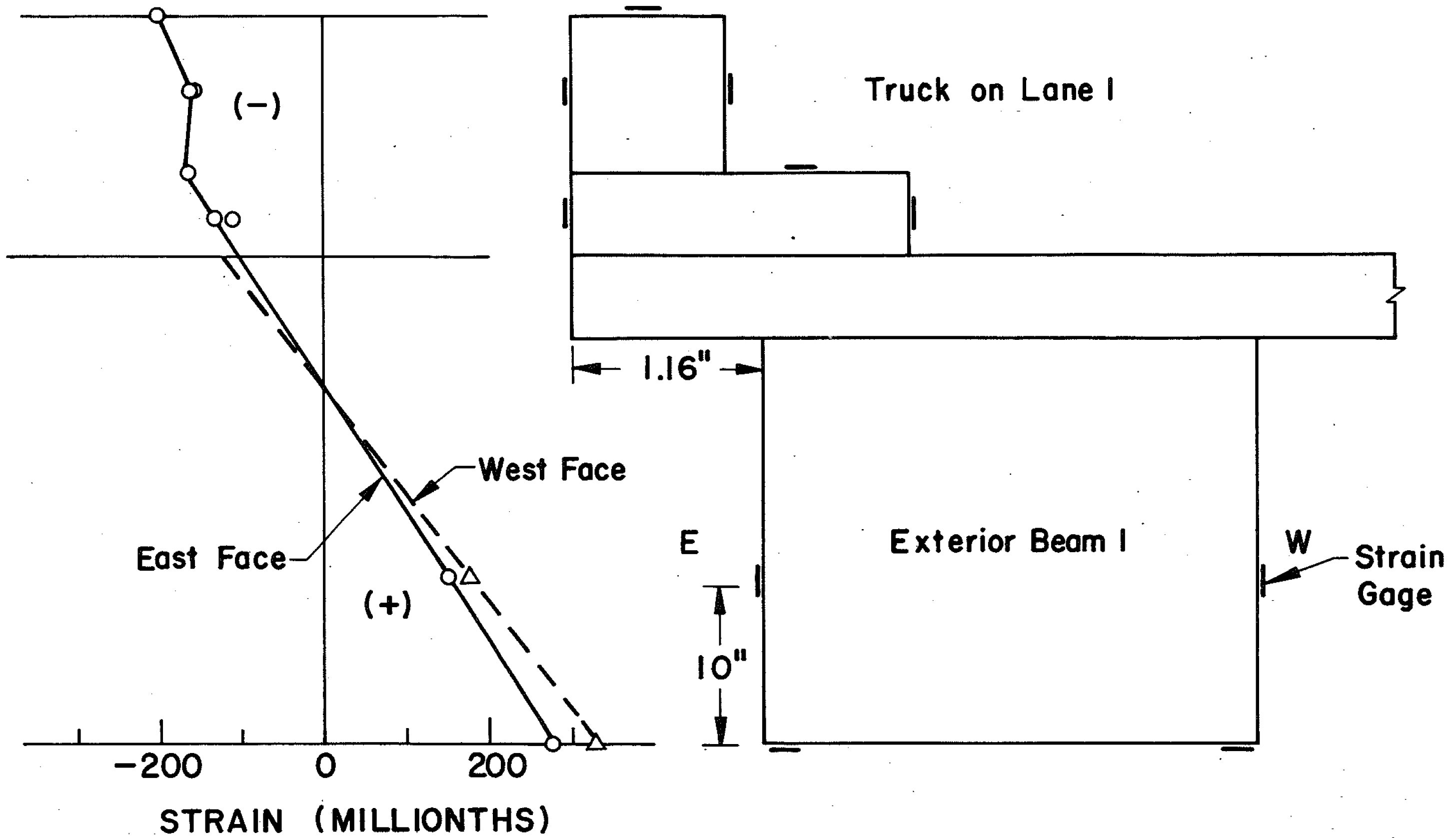

Fig. 4 Strains in Exterior Beam, Model A1

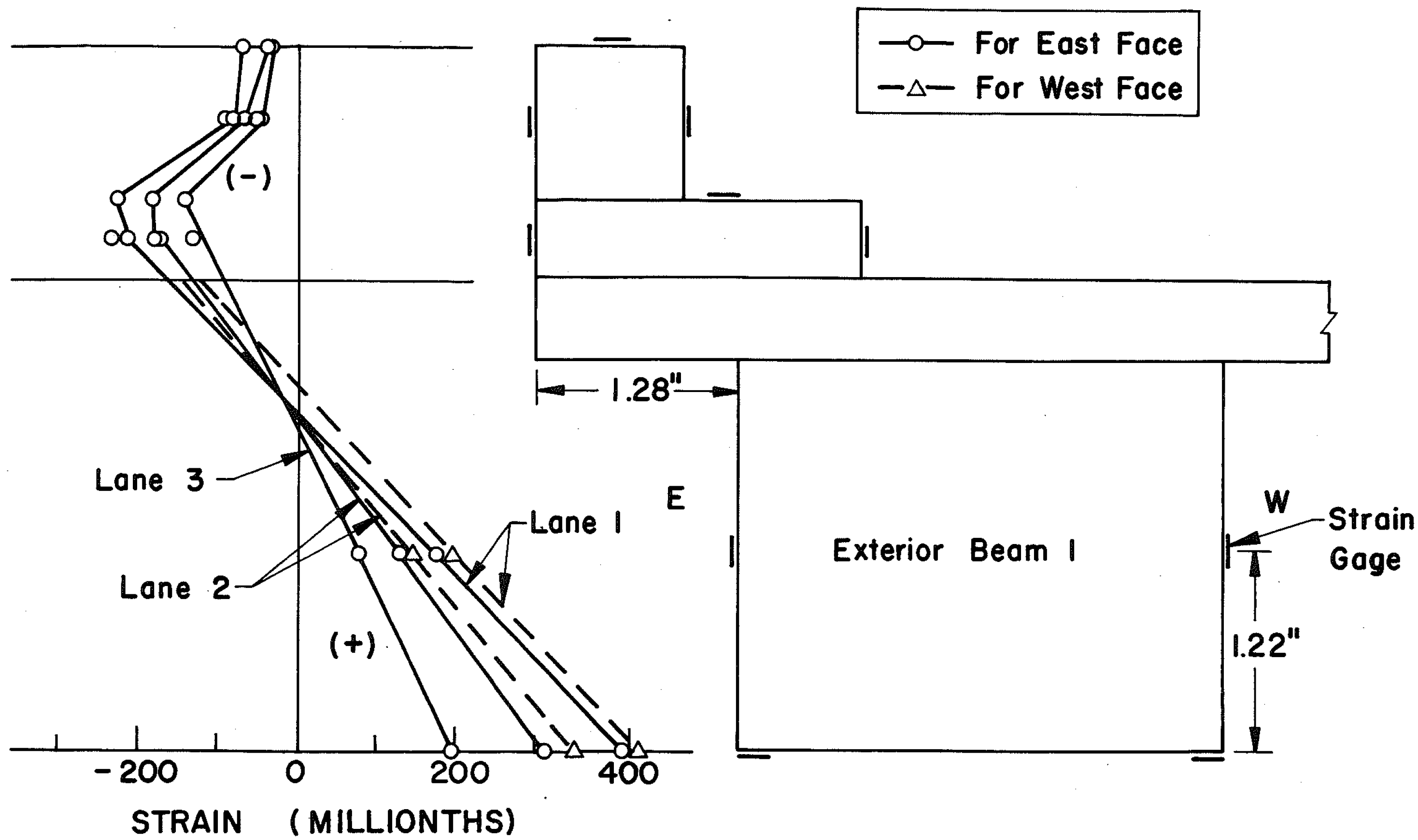

Fig. 5 Strains in Exterior Beam, Model B4

LOAD ON LANE	ROTATION OF NEUTRAL AXIS (RADIANS)			
	θ_1	θ_2	θ_3	θ_4
1	0.0268	0.0669	0.0836	0.0698
2	-0.0106	0.0282	0.0511	0.1392
3	-0.0892	0.0124	-0.0124	0.0898

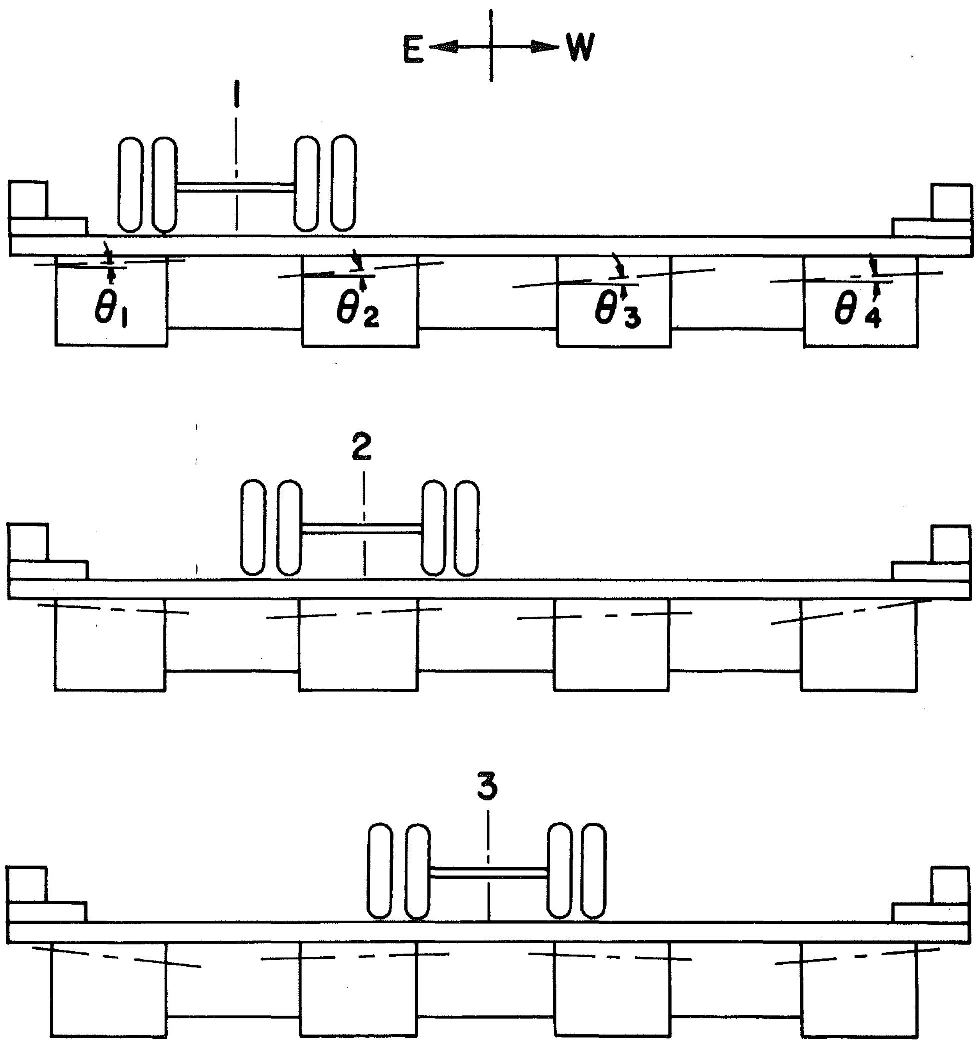

Fig. 6 Neutral Axes, Model A1

LOAD ON LANE	ROTATION OF NEUTRAL AXIS (RADIANS)			
	θ_1	θ_2	θ_3	θ_4
1	0.0725	0.1203	0.1885	0.2408
2	0.0409	0.0559	0.1549	0.1750
3	-0.0221	0.0236	0.0236	0.0221

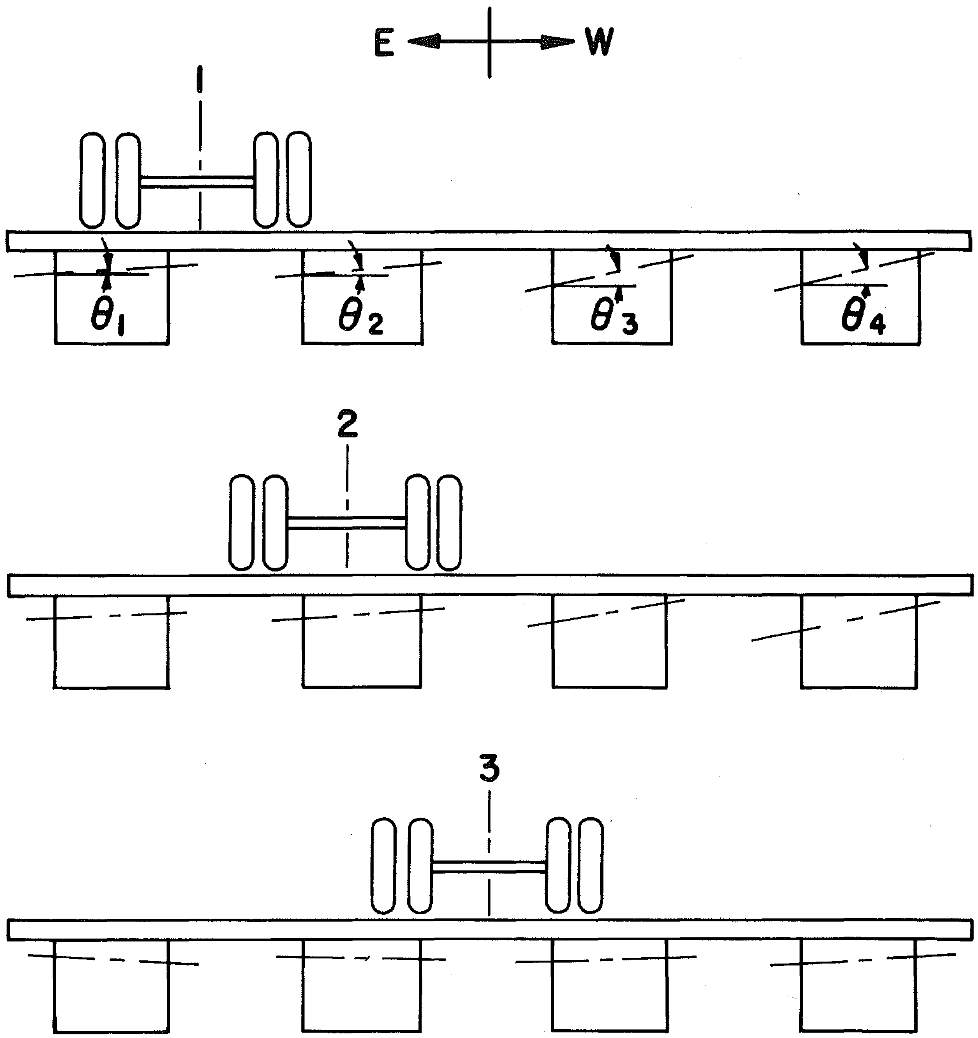

Fig. 7 Neutral Axes, Model B1

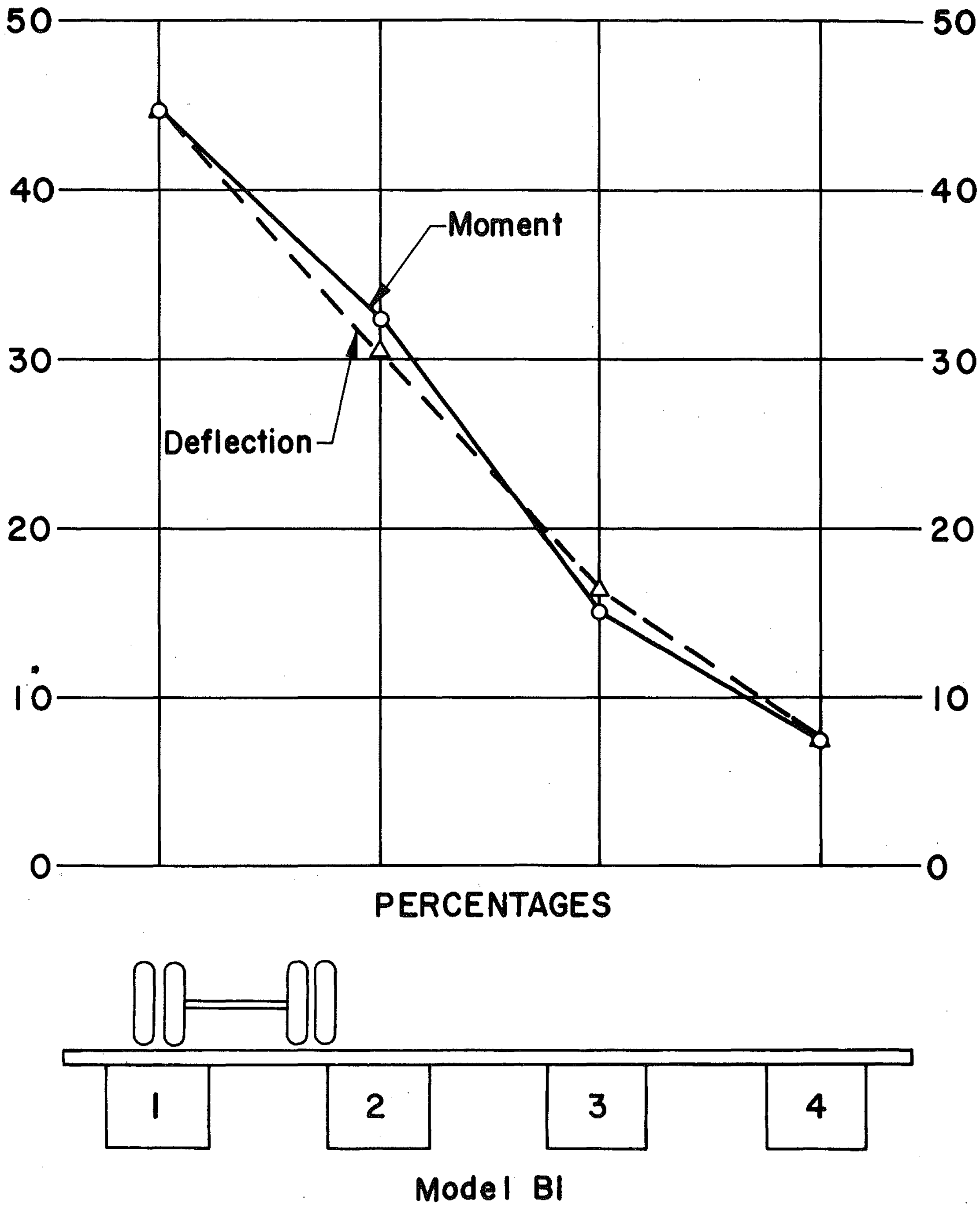

Fig. 8 Model B1, Lane 1

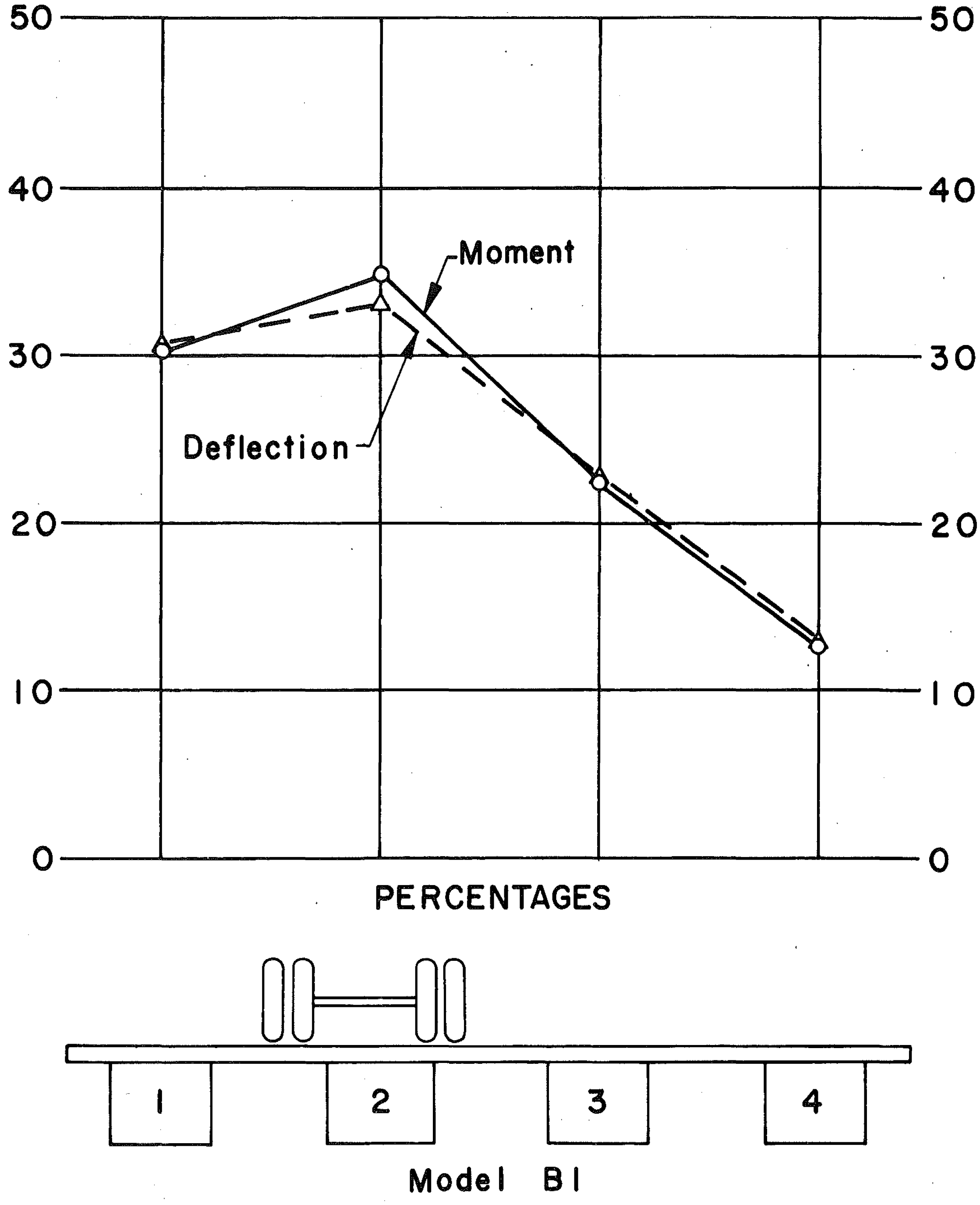

Fig. 9 Model B1, Lane 2

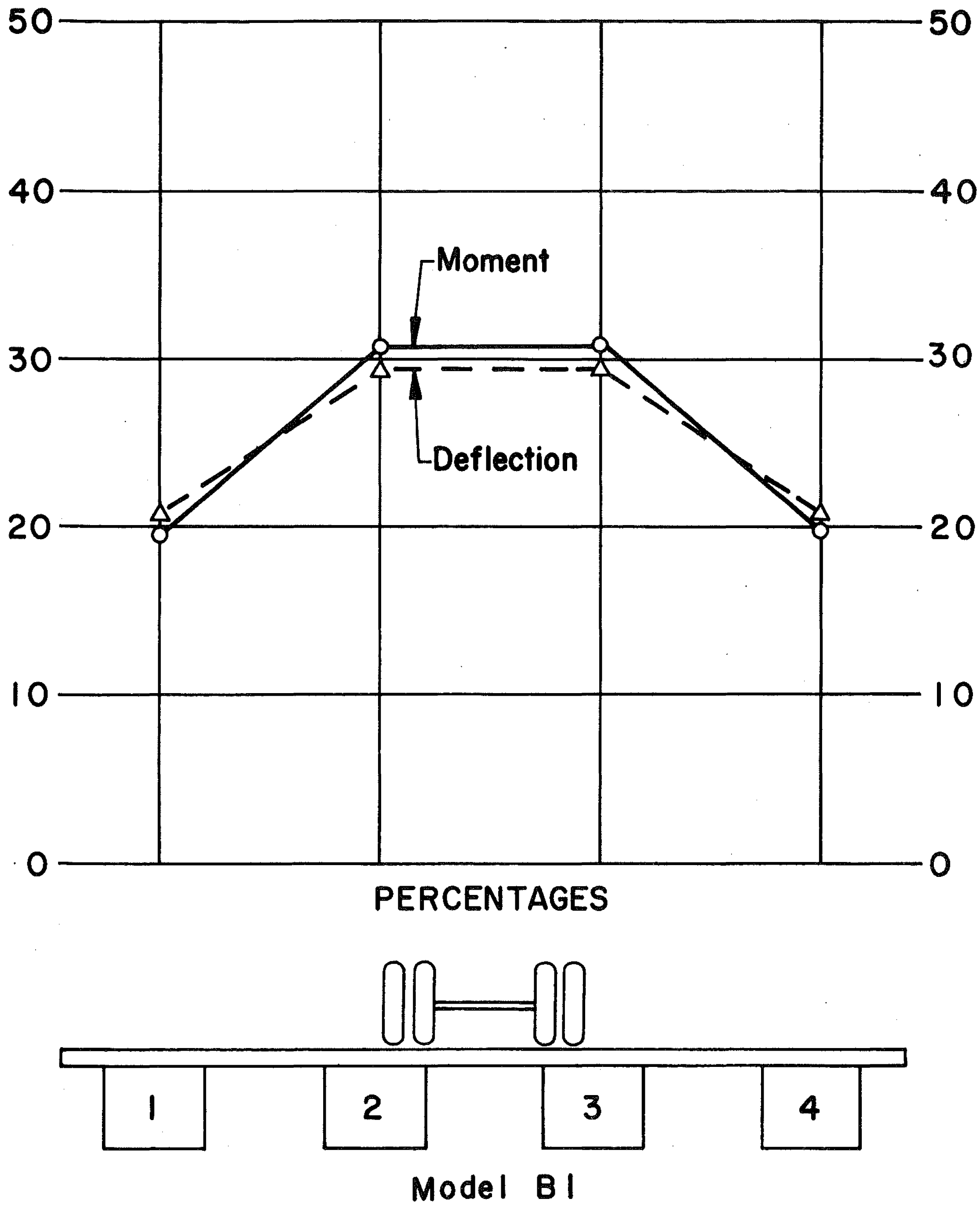

Fig. 10 Model B1, Lane 3

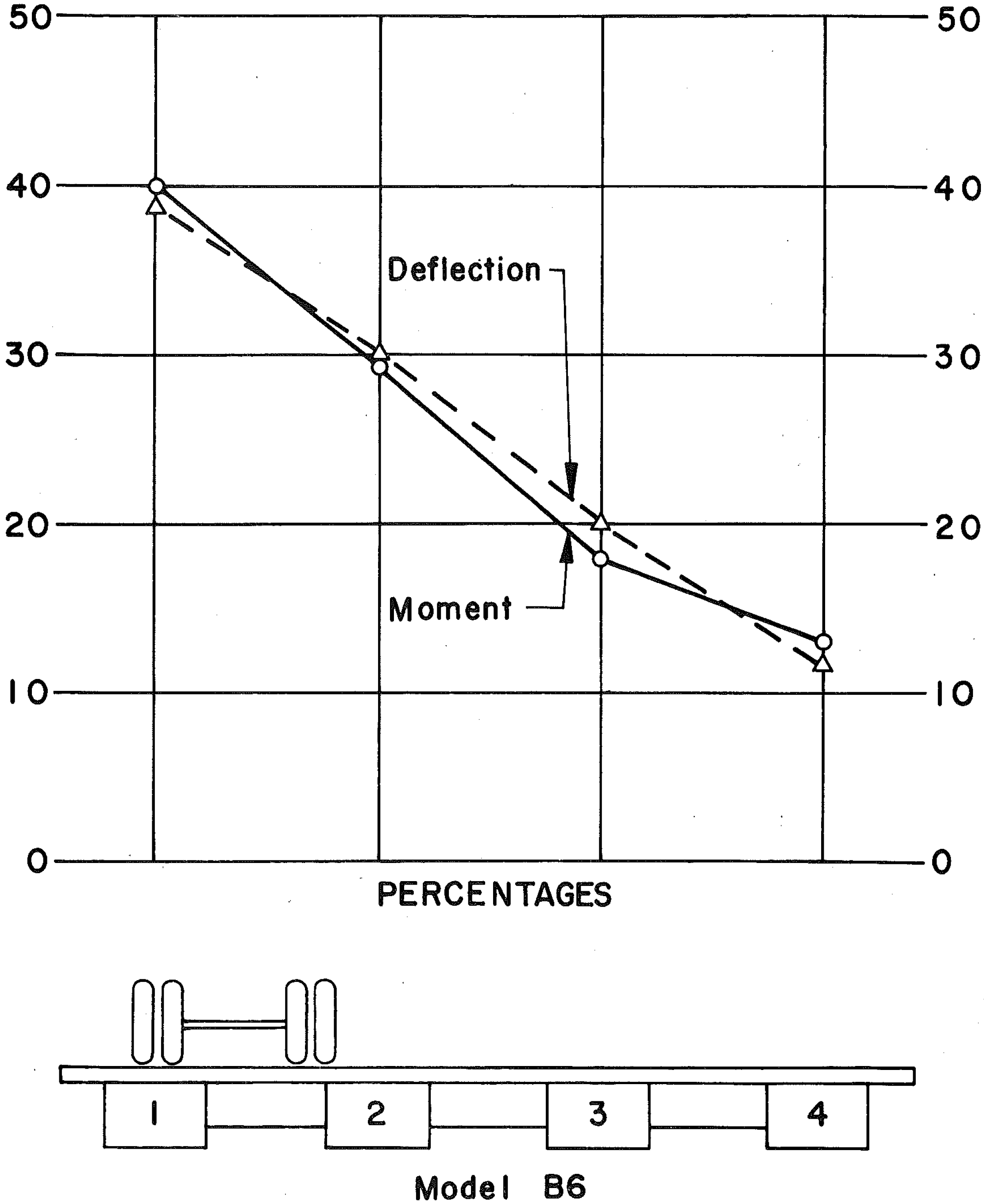

Fig. 11 Model B6, Lane 1

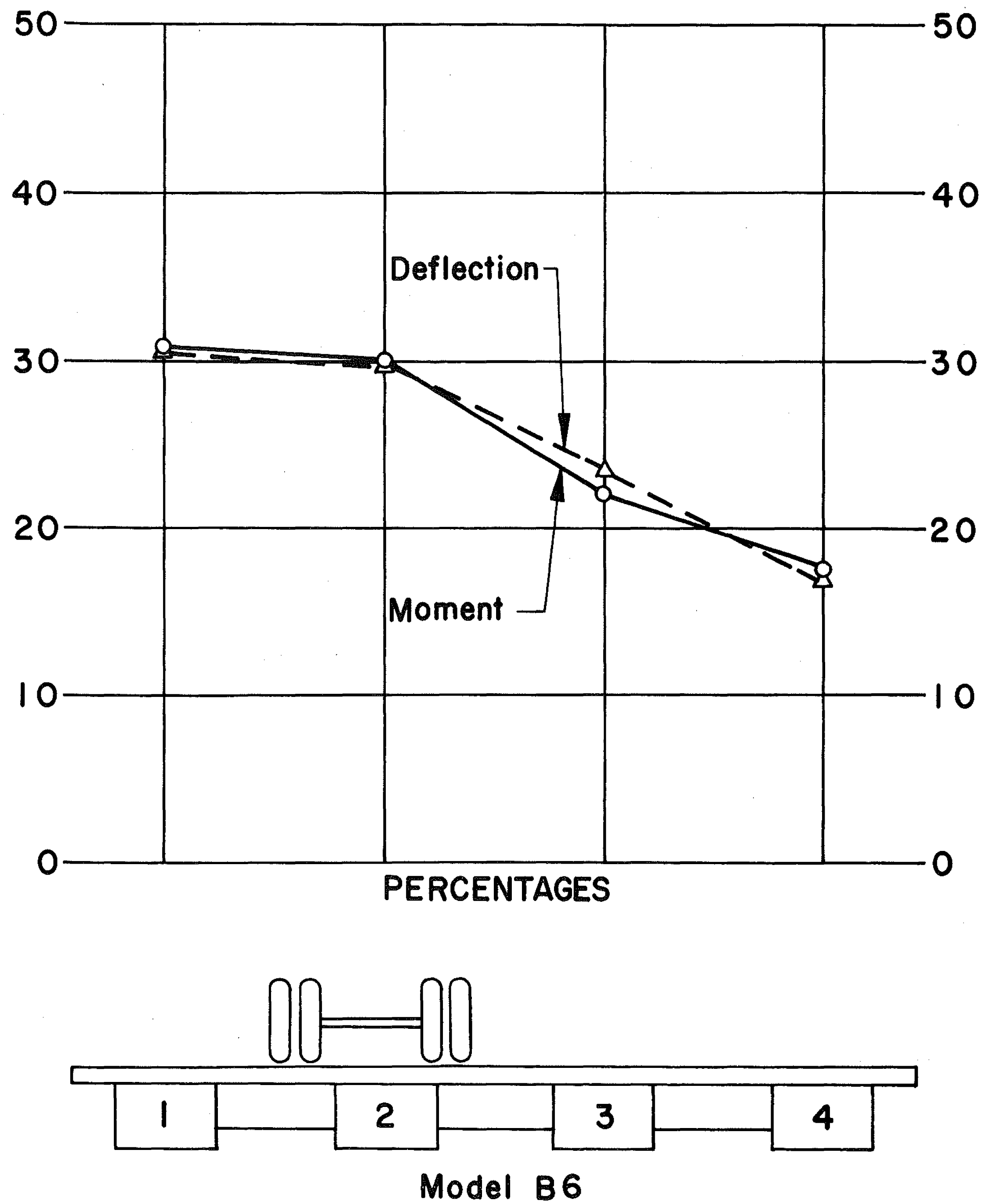

Fig. 12 Model B6, Lane 2

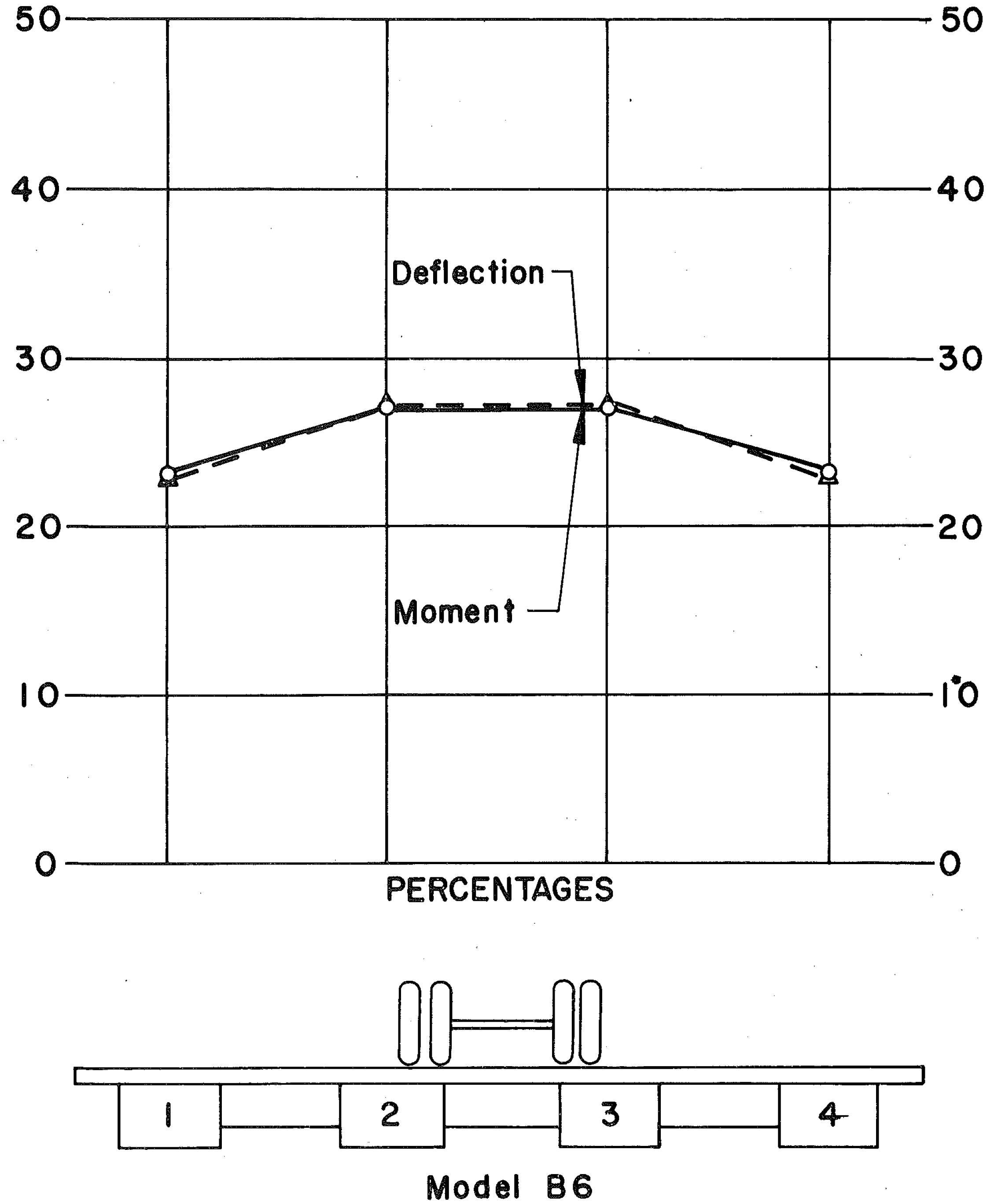

Fig. 13 Model B6, Lane 3

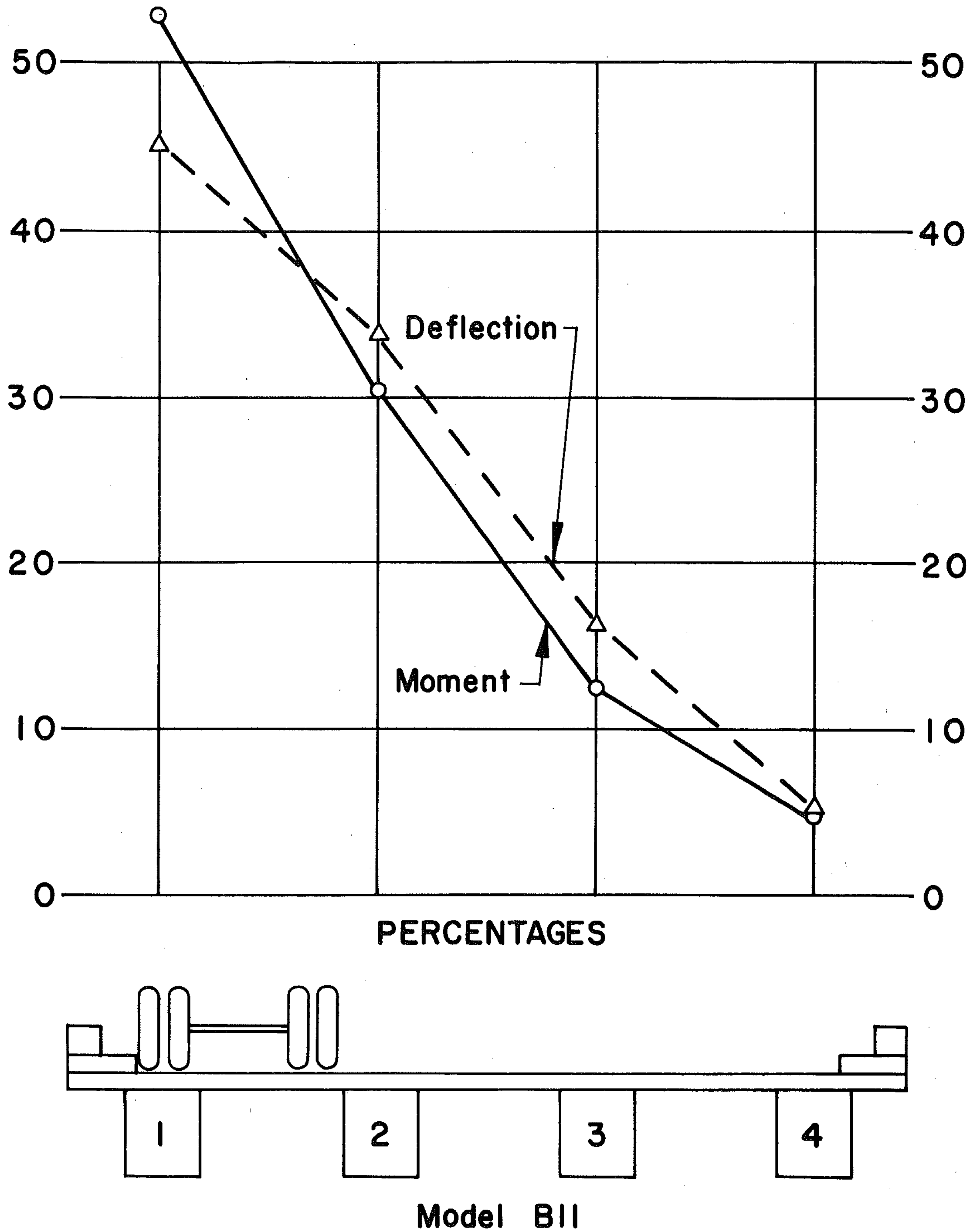

Fig. 14 Model B11, Lane 1

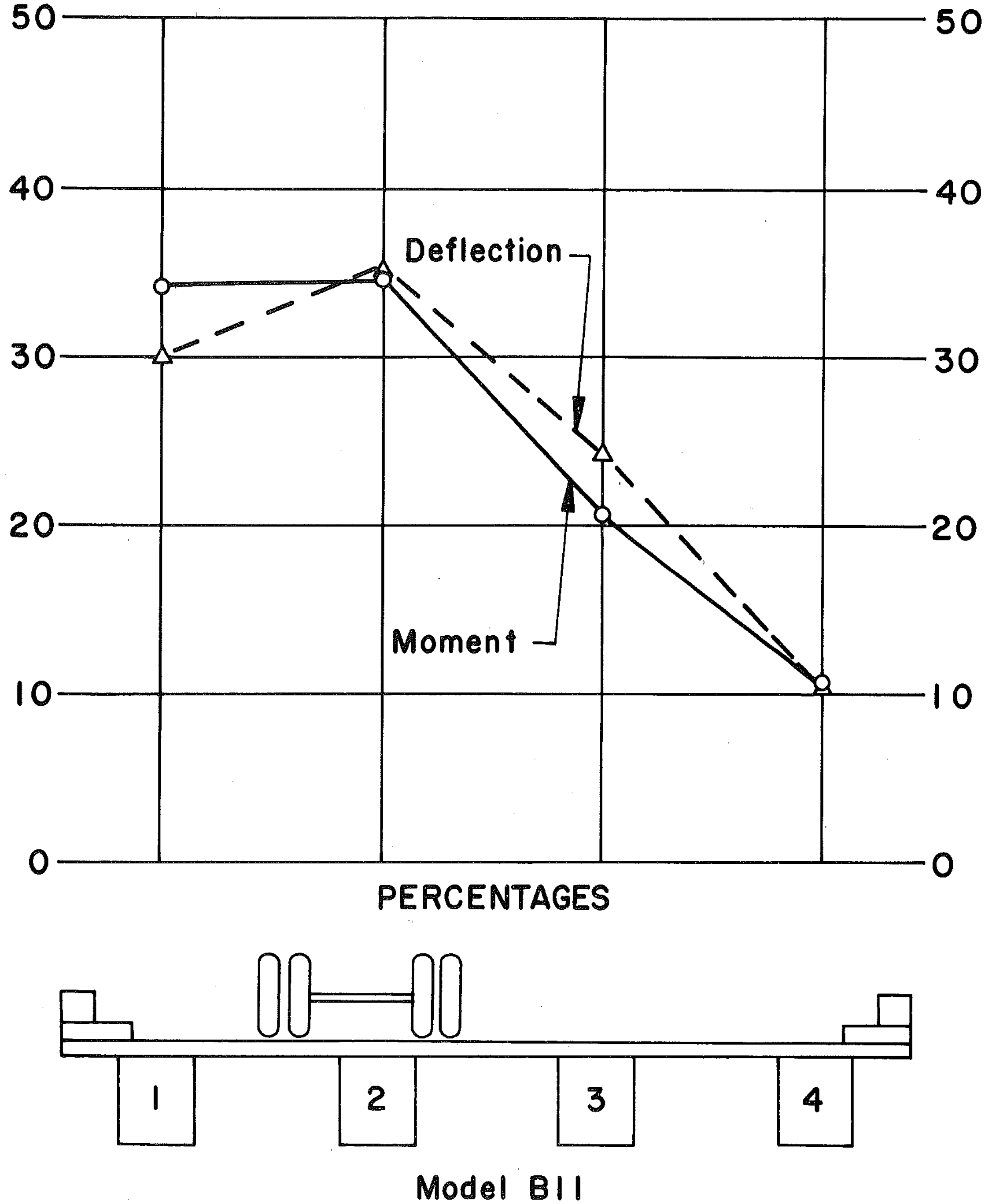

Fig. 15 Model B11, Lane 2

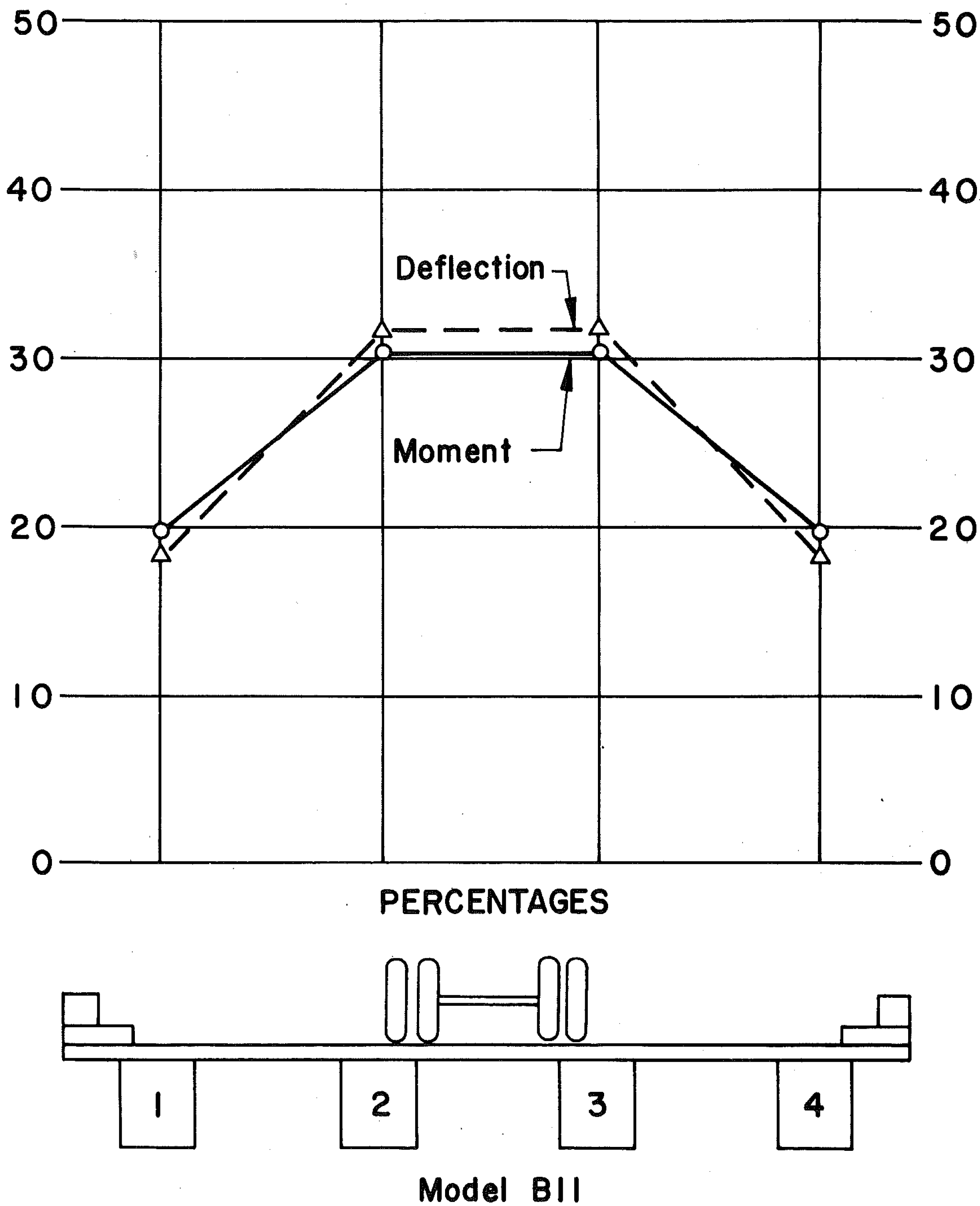

Fig. 16 Model B11, Lane 3

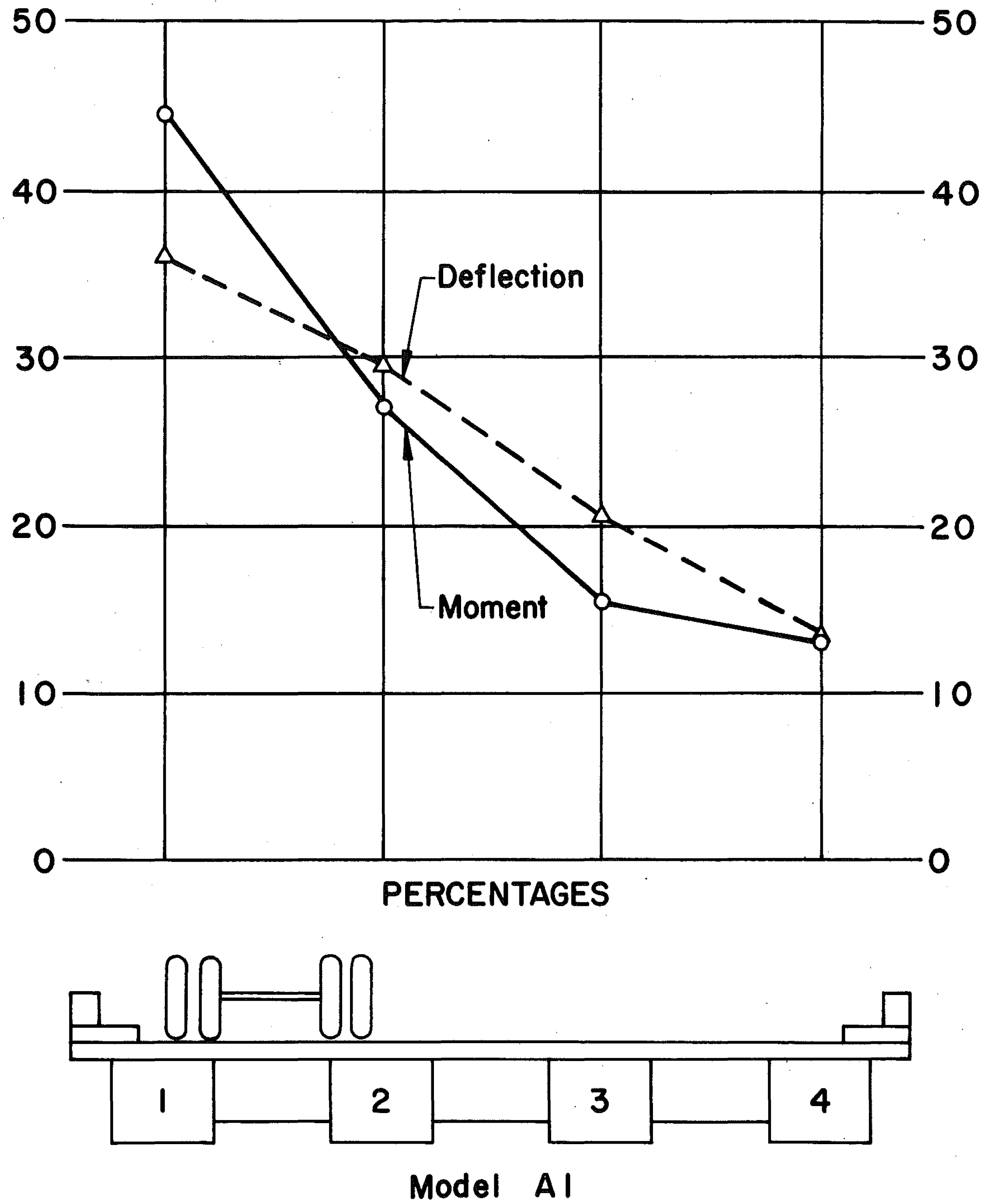

Fig. 17 Model A1, Lane 1

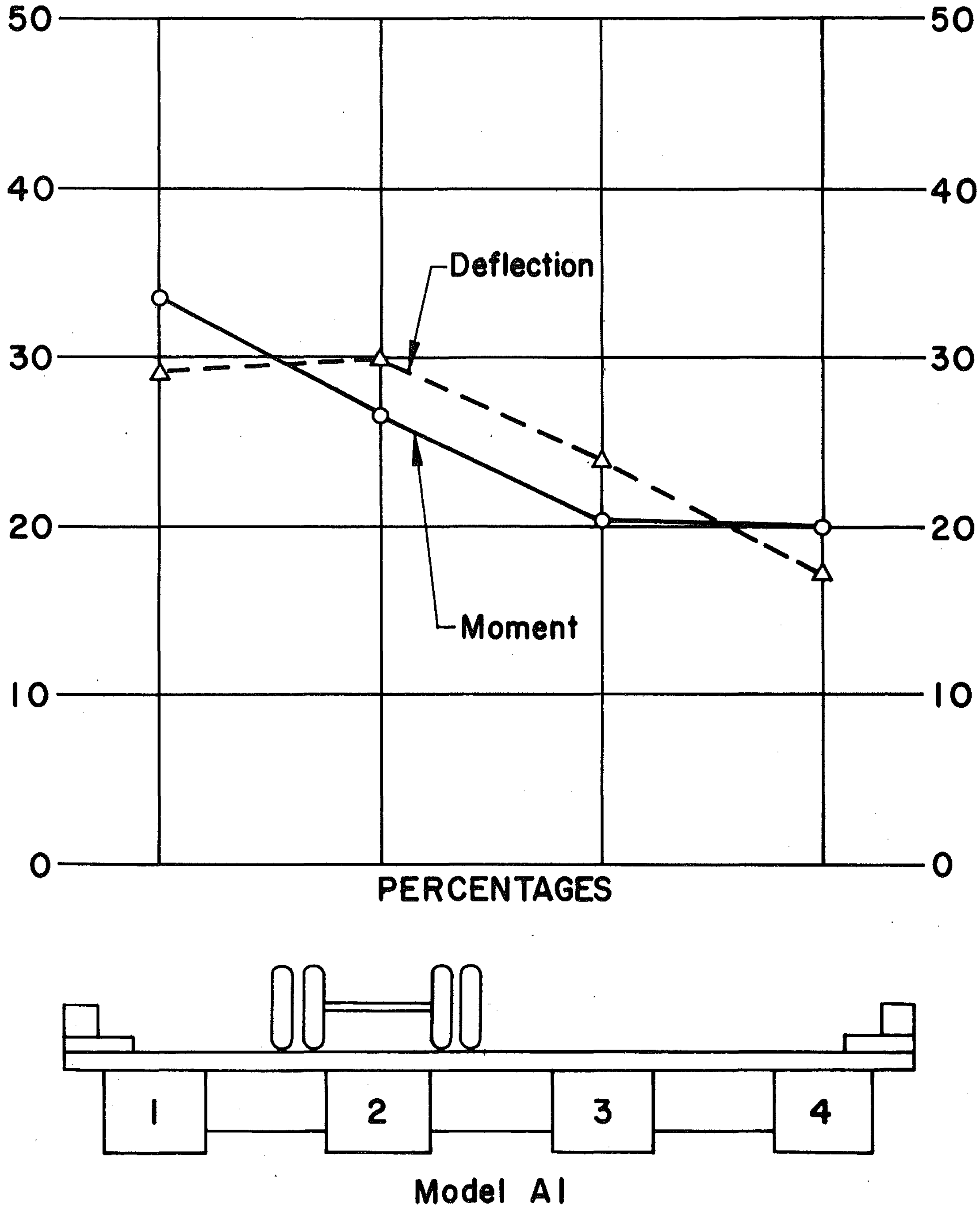

Fig. 18 Model A1, Lane 2

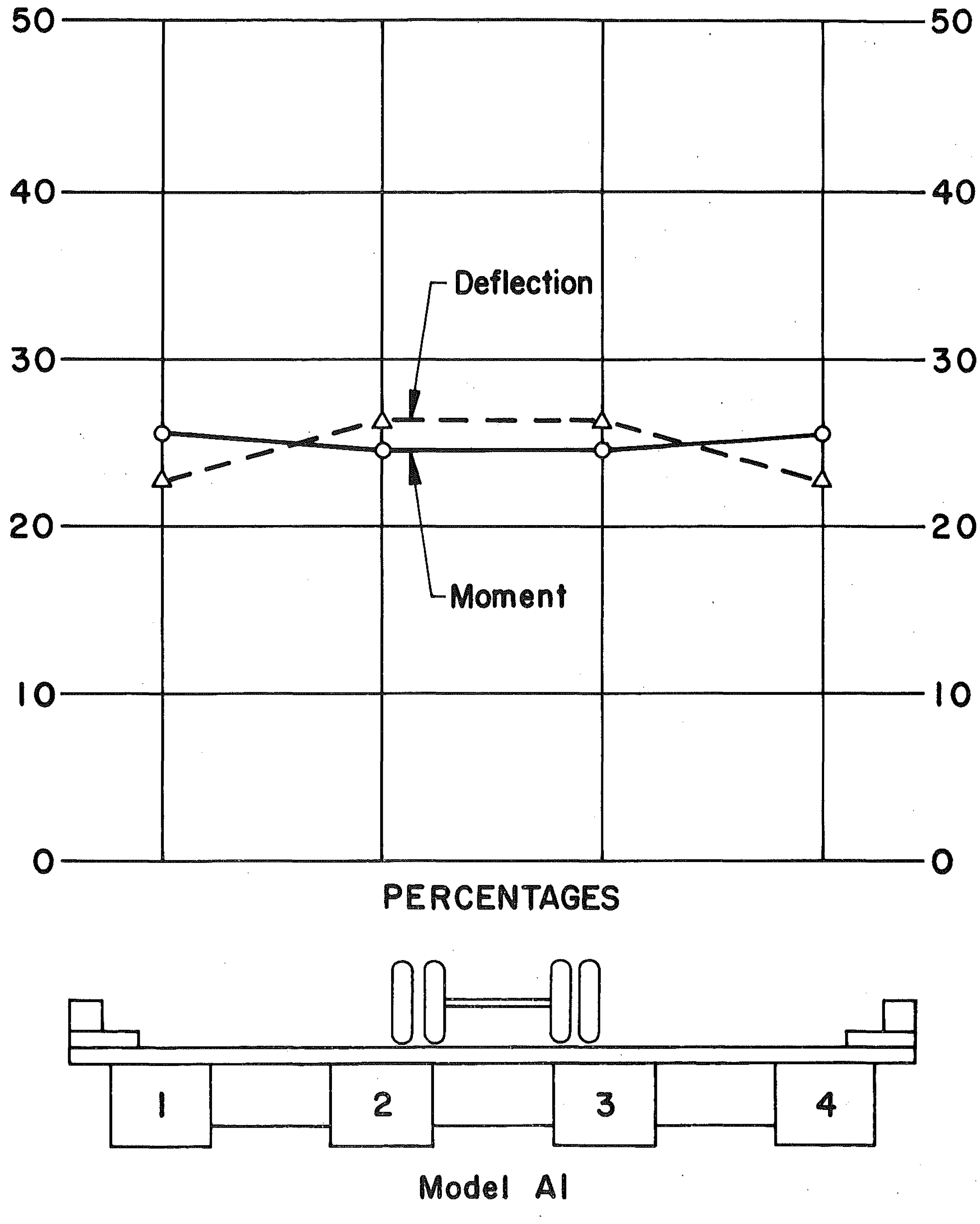

Fig. 19 Model A1, Lane 3

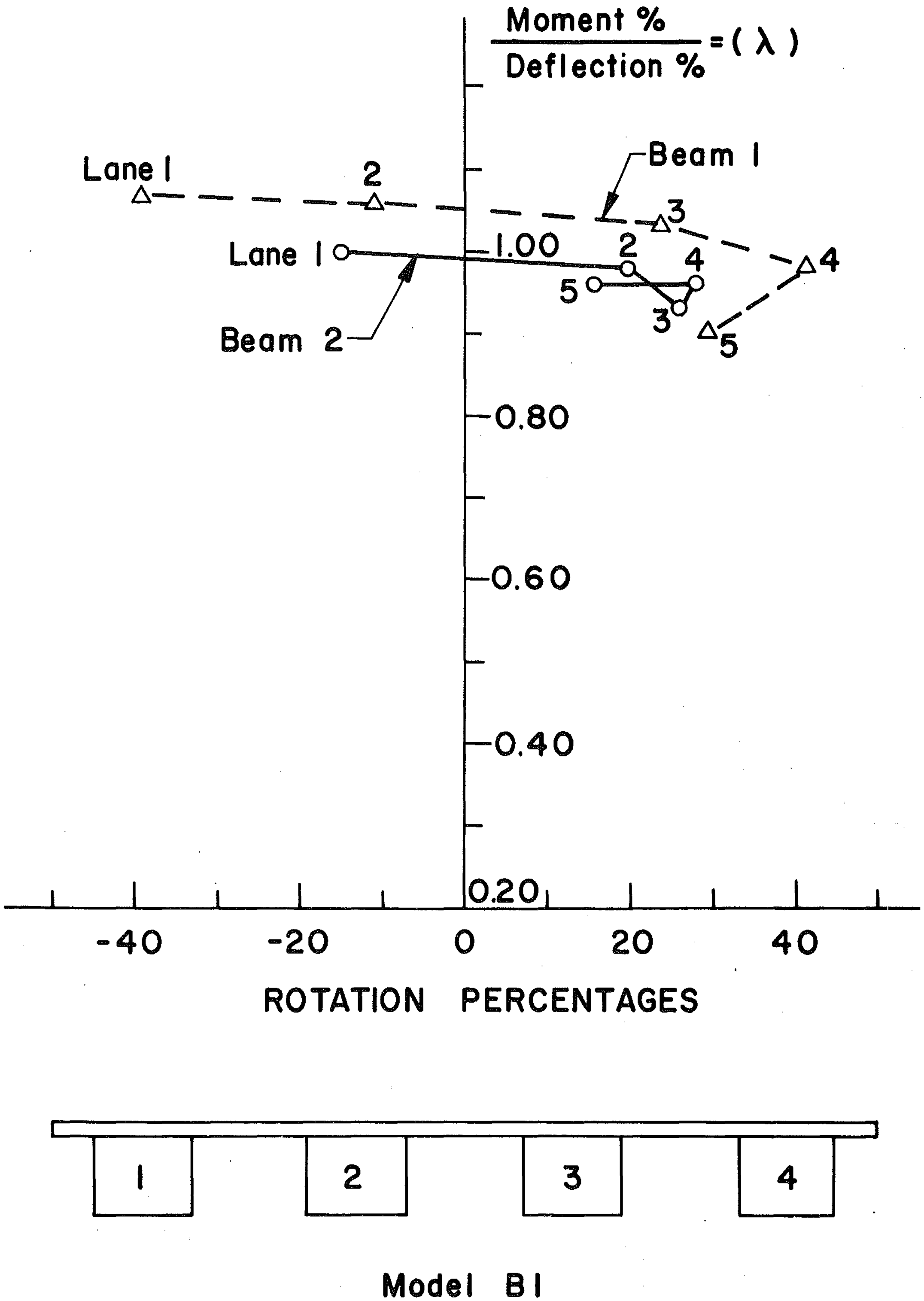

Fig. 20 Rotations, Model B1

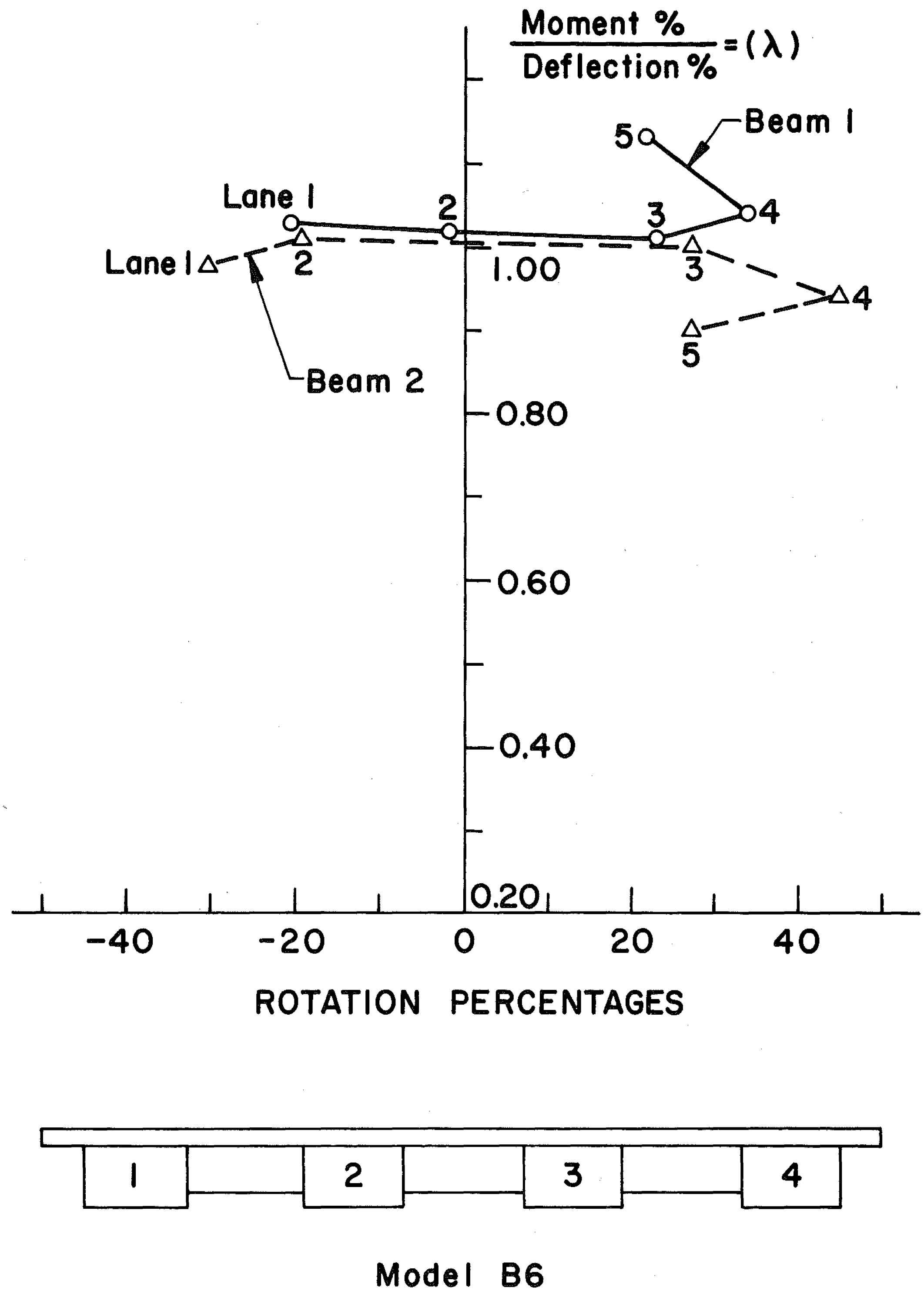

Fig. 21 Rotations, Model B6

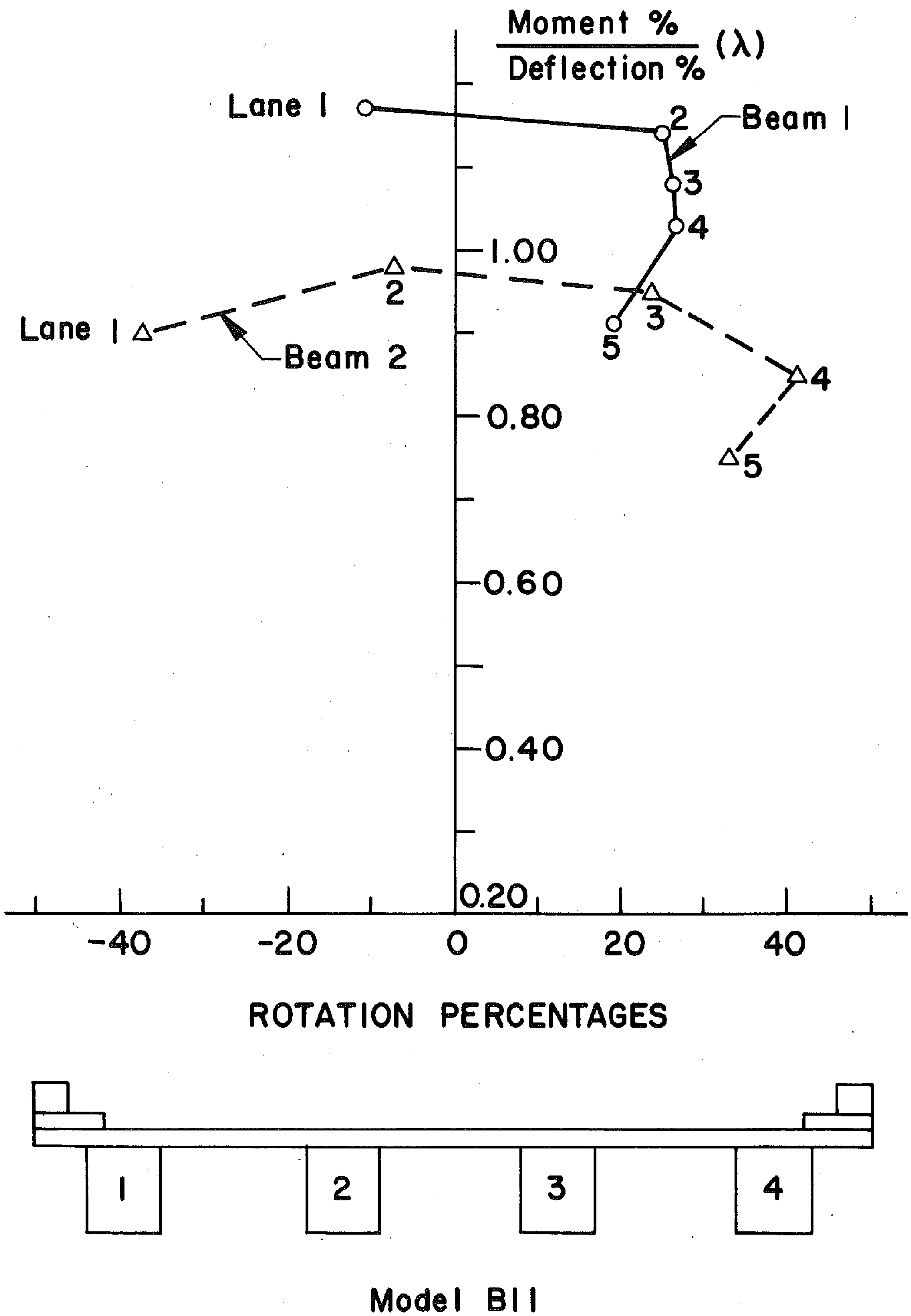

Fig. 22 Rotations, Model B11

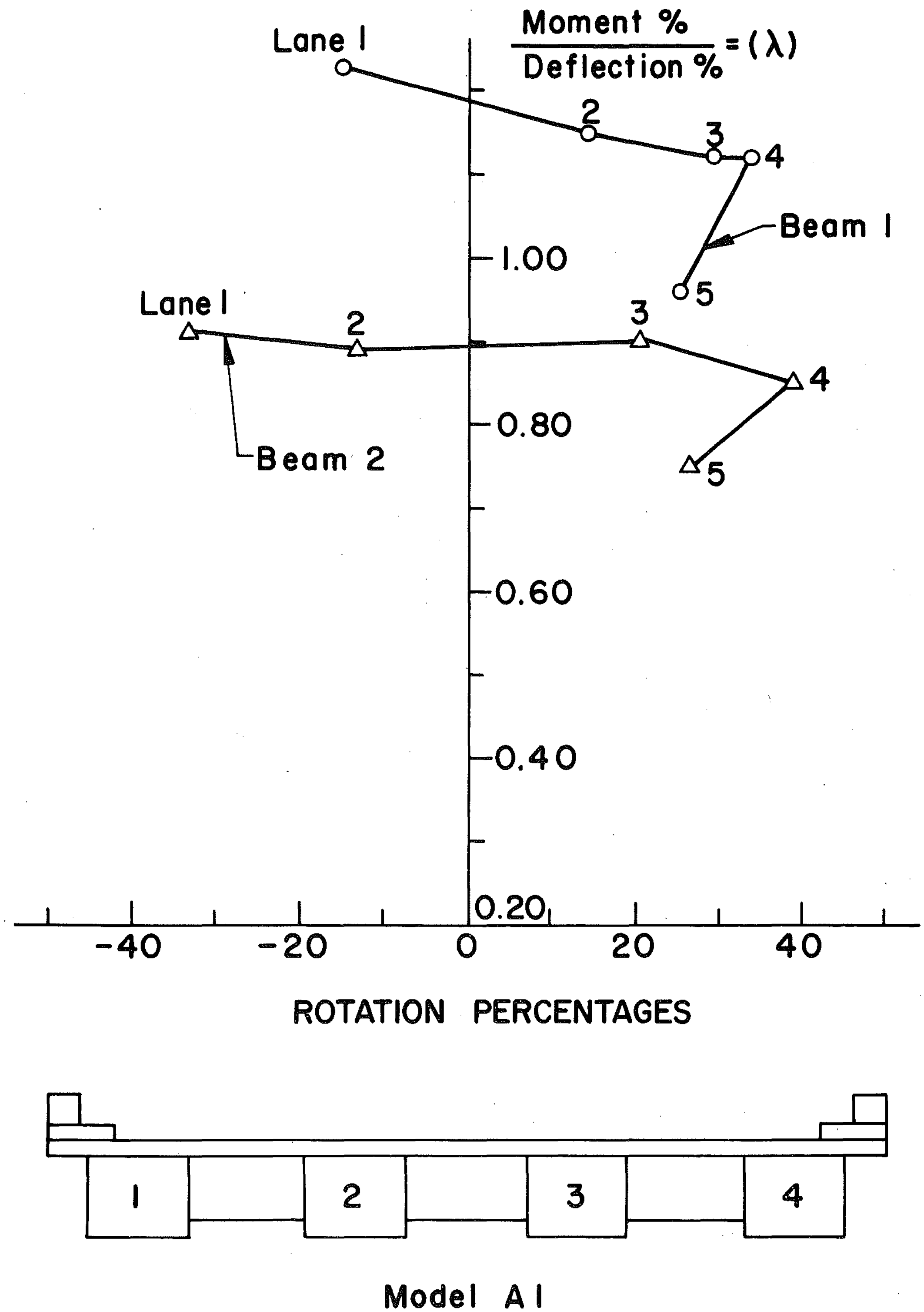

Fig. 23 Rotations, Model A1

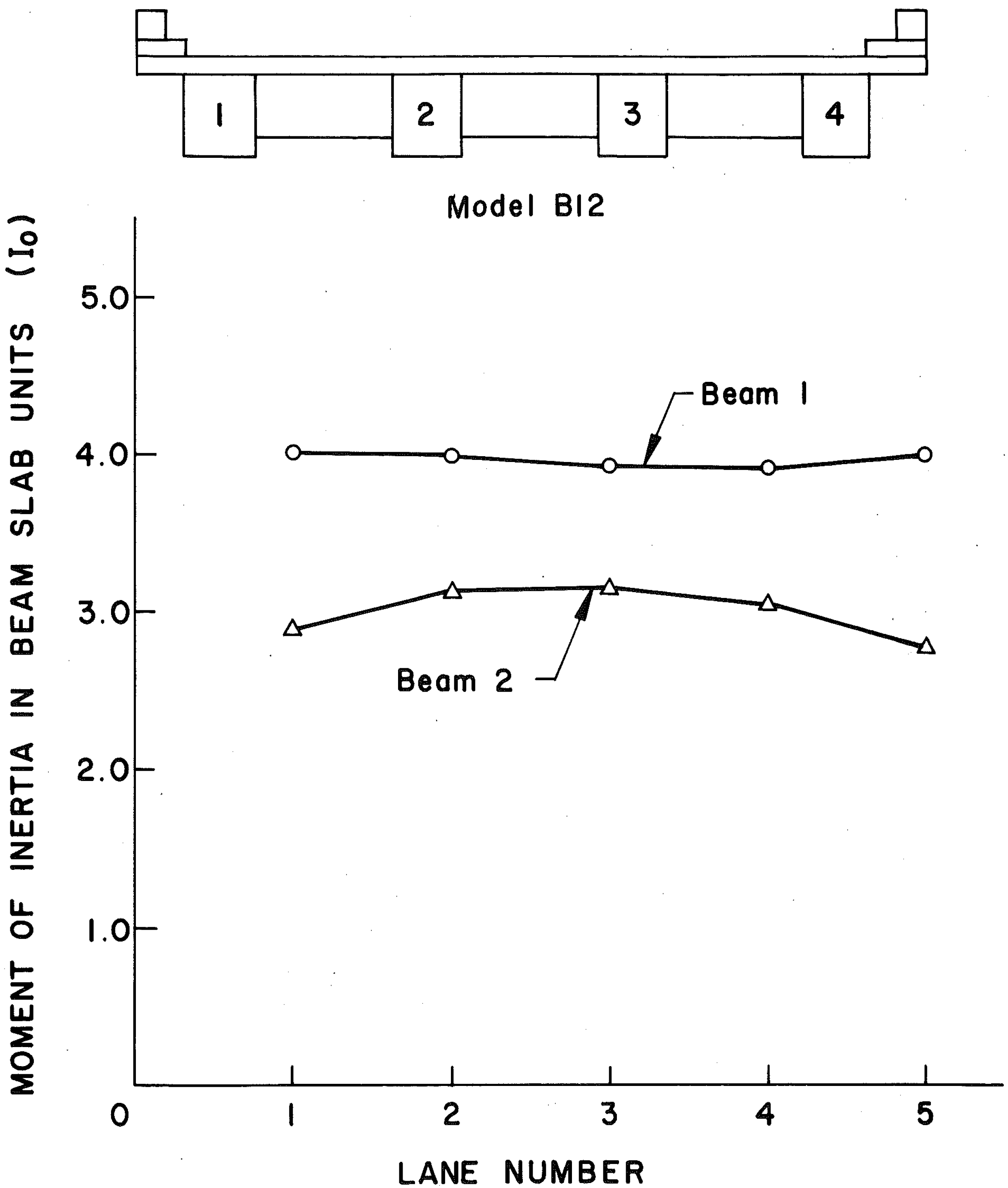

Fig. 24 Moments of Inertia, Model A1

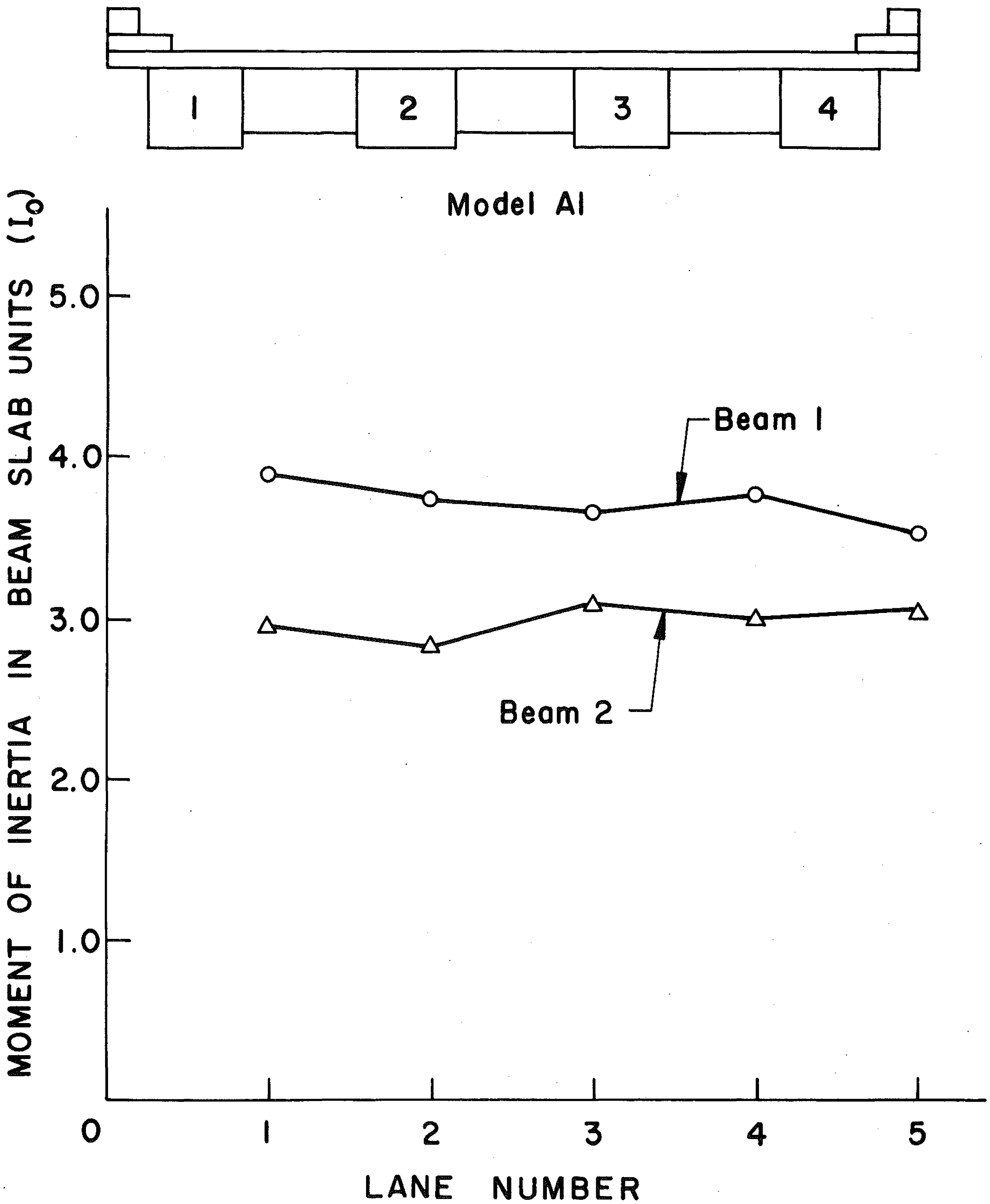

Fig. 25 Moments of Inertia, Model B12

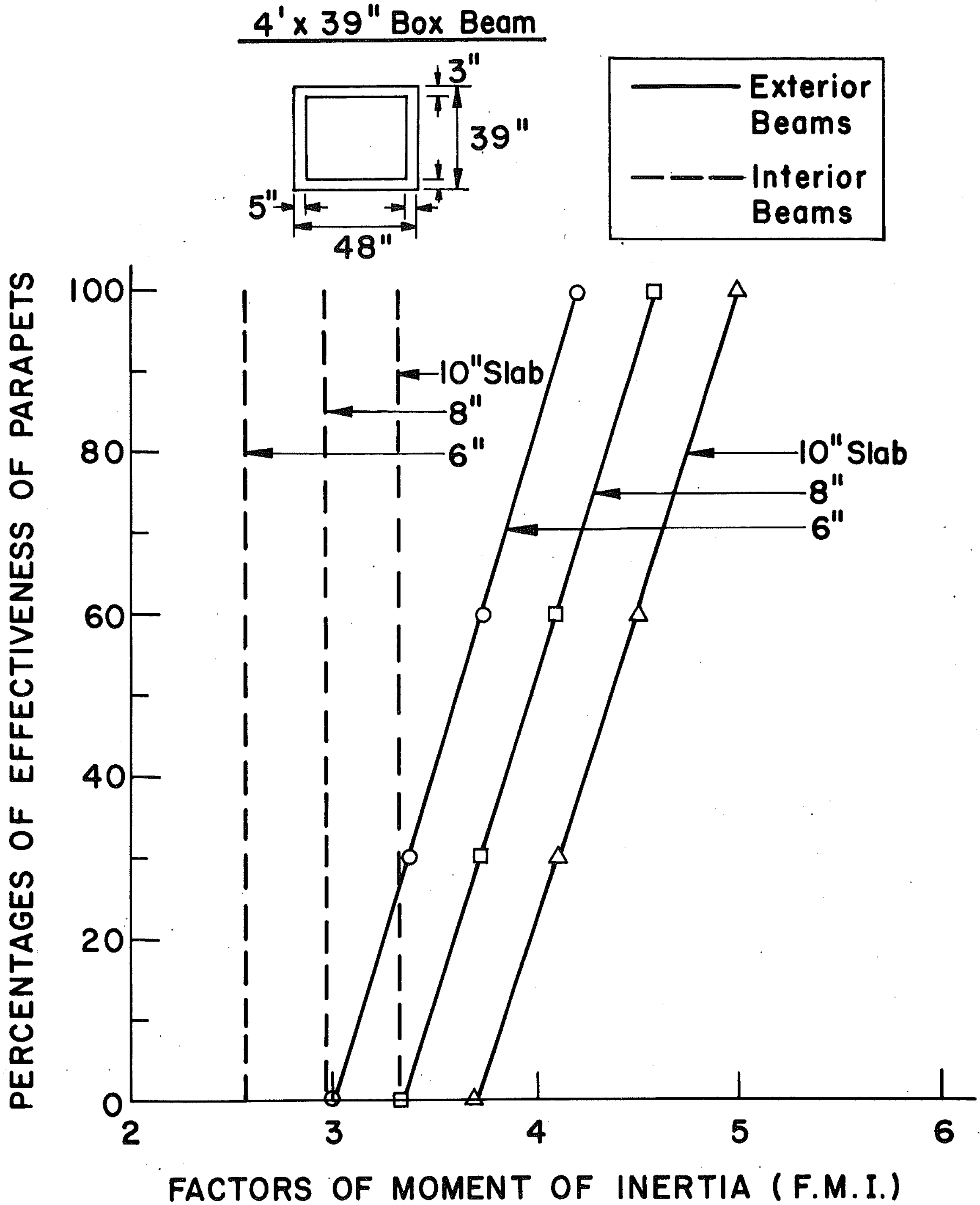

Fig. 26 F.M.I. Chart, 4 ft. x 39 in. Box Beam

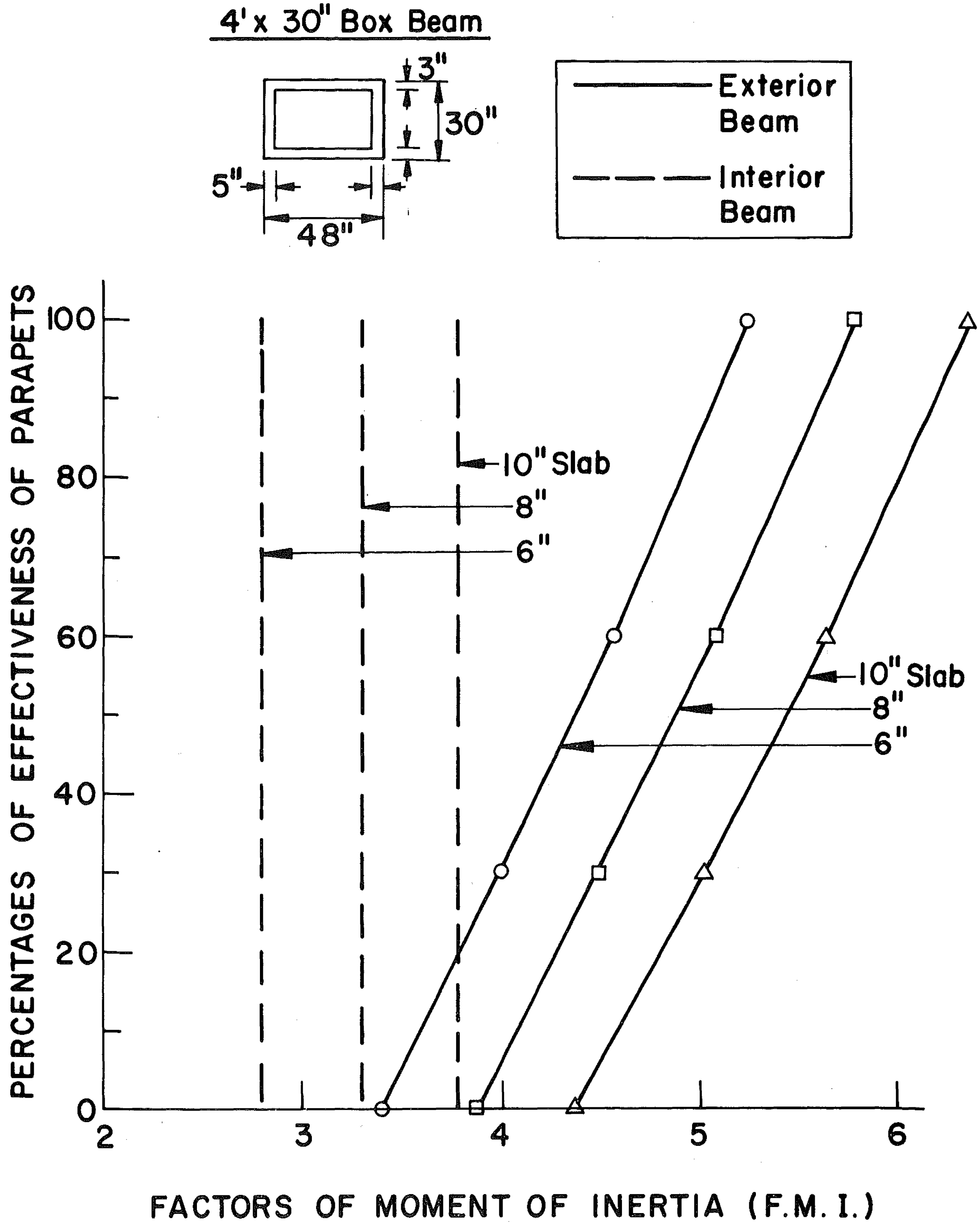

Fig. 27 F.M.I. Chart, 4 ft. x 30 in. Box Beam

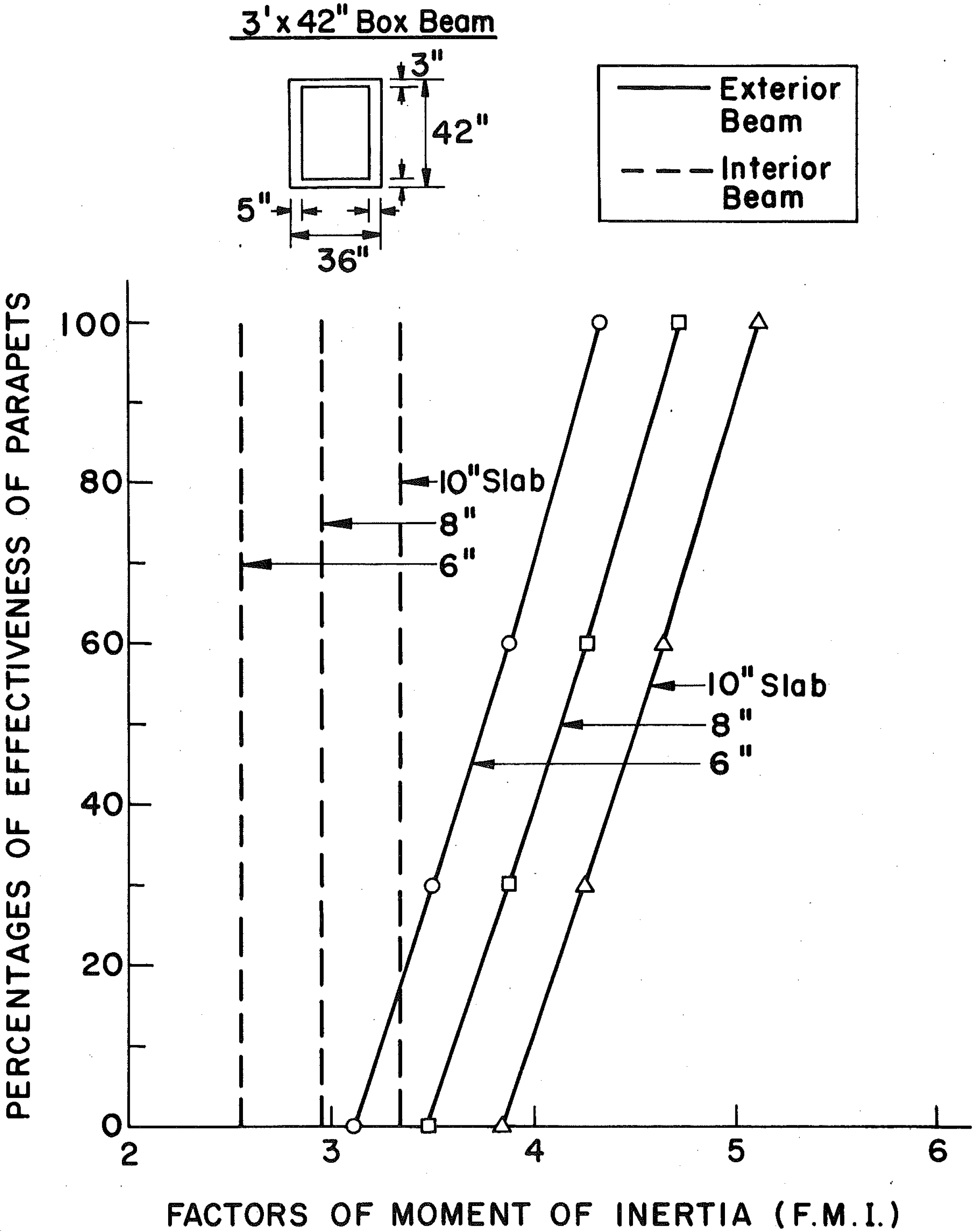

Fig. 28 F.M.I. Chart, 3 ft. x 42 in. Box Beam

10. REFERENCES

1. American Association of State Highway Officials
   STANDARD SPECIFICATIONS FOR HIGHWAY BRIDGES, Ninth Edition, Washington, D. C., 1965

2. Carpenter, J. E.
   STRUCTURAL MODEL TESTING; COMPENSATION FOR TIME EFFECT IN PLASTICS, Portland Cement Association, Skokie, Illinois, Bull. D60, January 1963

3. Carpenter, J. E., Magura, D. D., and Hanson, N. W.
   STRUCTURAL MODEL TESTING; TECHNIQUES FOR MODELS OF PLASTIC, Portland Cement Association, Skokie, Illinois, Bull. D76, May 1964

4. Carpenter, J. E. and Magura, D. D.
   STRUCTURAL MODEL TESTING; LOAD DISTRIBUTION IN CONCRETE I-BEAM BRIDGES, Portland Cement Association, Skokie, Illinois, Bull. D94, September 1965

5. Guilford, A. A. and VanHorn, D. A.
   LATERAL DISTRIBUTION OF VEHICULAR LOADS IN A PRE-STRESSED CONCRETE BOX-BEAM BRIDGE, BERWICK BRIDGE, Fritz Engineering Laboratory Report No. 315.4, Lehigh University, October 1967

6. Hondros, G. and Marsh, J. G.
   LOAD DISTRIBUTION IN COMPOSITE GIRDER-SLAB BRIDGES, ASCE Journal of Structural Division, Vol. 86, No. ST11, New York, November 1960

7. Little, G.
   DISTRIBUTION OF A LOAD IN A BOX-SECTION BRIDGE FROM TESTS ON A XYLONITE MODEL, Magazine of Concrete Research, Vol. 6, No. 18, London, December 1954

8. Little, G. and Rowe, R. E.
   LOAD DISTRIBUTION IN MULTI-WEBBED BRIDGE STRUCTURES FROM TESTS ON PLASTIC MODELS, Magazine of Concrete Research, Vol. 7, No. 21, London, November 1955

9. Macías Rendón, M. A.
A STRUCTURAL MODEL STUDY OF LOAD DISTRIBUTION IN BOX-BEAM BRIDGES, Ph.D. Dissertation, Lehigh University, May 1968

10. Massonnet, C.
METHODE DE CALCUL DES PONTS A POUTRES MULTIPLES TENANT COMPTE DE LEUR RESISTANCE A LA TORSION, (Method of Calculation for Bridges With Several Longitudinal Beams, Taking Into Consideration Their Torsional Resistance), Publications, IABSE, Zurich, Vol. 10, 1950

11. Mattock, A. H. and Kaar, P. H.
PRECAST-PRESTRESSED CONCRETE BRIDGES 6. TESTS OF HALF-SCALE HIGHWAY BRIDGE CONTINUOUS OVER TWO SPANS, Portland Cement Association, Skokie, Illinois, Bull. D51, September 1961

12. Newmark, N. M.
DISTRIBUTION PROCEDURE FOR ANALYSIS OF SLABS OVER FLEXIBLE SUPPORTS, University of Illinois Engineering Experimental Station Bulletin No. 304, June 1938

13. Pennsylvania Department of Highways
STANDARDS FOR PRESTRESSED CONCRETE BRIDGES, ST-200 through ST-208, Harrisburg, Pennsylvania, 1964

14. Reese, R. T.
LOAD DISTRIBUTION IN HIGHWAY BRIDGE FLOORS: A SUMMARY AND EXAMINATION OF EXISTING METHODS OF ANALYSIS AND DESIGN AND CORRESPONDING RESULTS, Brigham Young University, M.S. Thesis, 1966

15. Richart, F. E.
LABORATORY RESEARCH ON CONCRETE BRIDGE FLOORS, Highway Bridge Floors, A Symposium, ASCE Proceedings, Part 1, March, 1948

16. Roll, F. and Aneja, I.
MODEL TESTS OF BOX-BEAM HIGHWAY BRIDGES WITH CANTILEVERED DECK SLABS, ASCE Transportation Engineering Conference Reprint No. 395, Philadelphia, Pennsylvania, October 1966

17. Rowe, R. E.
CONCRETE BRIDGE DESIGN, John Wiley and Sons, Inc., New York, 1962

18. Stevens, L. K. and Gosbell, K. B.
MODEL ANALYSIS OF A COMPOSITE BEAM AND SLAB BRIDGE, Australian Road Research Board Proceedings, Vol. 2, 1964

19. Westlund, G. and Ostlund, L.
TESTS ON A BRIDGE MODEL, Publications, IABSE, Zurich, 1950